

# Impact of Climatic Controls on Global Changes in Land Surface Phenology

GEO 511: Masterarbeit

24 September 2015

David Schenkel

10-721-272

Supervisors:

Dr. Rogier de Jong

Irene Garonna, MSc

Prof. Dr. Michael E. Schaepman

Remote Sensing Laboratories

Department of Geography, University of Zurich

## Abstract

Land Surface Phenology (LSP) plays an important role in global vegetation–climate feedback loops. Satellite observations have shown global shifts of the Start Of Season (SOS), Growing Season Length (GSL) and End Of Season (EOS) in the past decades. Understanding the role of climatic factors on these changes is an important step towards a better understanding of the effects climate change will have in the future. Models based on climatic factors limiting LSP, so called climatic controls (temperature, moisture and radiation), have been created to simulate green-up and senescence in the form of Leaf Area Index (LAI) estimates. With the development of long-term time-series of remotely sensed LAI datasets, it has become possible to compare the modelled data to satellite observations and assess the impact changes in climatic controls had on global LSP in the past decades. In this thesis, a remotely sensed LAI based on the longest available global Normalized Difference Vegetation Index (NDVI) time-series is used to verify a modelled LAI based on the three climatic controls by comparing LSP trends from 1982–2011 extracted from both datasets. Then, changes in the dominating climatic controls as well as individual changes of controls over the last 30 years are examined. Lastly, extracted SOS and EOS trends are connected to climatic controls to study dominating controls during SOS and EOS and assess individual changes in climatic controls at SOS and EOS from 1982–2011. It was found that the modelled and measured LAI are very similar and produced matching results particularly for the SOS in the Northern Hemisphere. The EOS showed more variability, hinting at more complex processes underlying autumn phenology. Temperature was found to be a dominating climatic control for most of the Northern Hemisphere with a clear trend towards less limitation in the last 30 years. Moisture was shown to get more limiting globally, particularly in the Southern Hemisphere. Radiation was shown to become an increasingly important limitation as the SOS retreats in the Northern Hemisphere. The results indicate that with rising temperatures, limitations due to moisture availability and radiation become more important for global vegetation dynamics and its effects need a better understanding to simulate future scenarios.

# Table of Contents

Abstract .....	i
Table of Contents .....	ii
List of Figures.....	iv
List of Tables.....	v
<b>1 Introduction.....</b>	<b>1</b>
<b>2 Data &amp; Methods .....</b>	<b>3</b>
2.1 Leaf Area Index datasets.....	3
2.1.1 LAIre – Modelled LAI.....	3
2.1.2 LAI3g – Measured LAI.....	4
2.2 Methods.....	4
2.2.1 Data Pre-processing .....	4
2.2.2 Extraction of Land Surface Phenological Parameters .....	5
2.2.3 Comparing LAIre to LAI3g.....	7
2.2.4 Trends in Climatic Controls.....	8
2.2.5 Influence of Climatic Controls on Land Surface Phenology.....	9
<b>3 Results .....</b>	<b>11</b>
3.1 Comparing LAIre to LAI3g.....	11
3.1.1 Raw LAI Data.....	11
3.1.2 LSP Parameters .....	11
3.1.3 Trends in SOS and EOS (1982 – 2011).....	13
3.2 Climatic Controls .....	14
3.2.1 Yearly Dominating Control.....	14
3.2.2 Quarterly Trends for Climatic Controls.....	14
3.3 Influence of Climatic Controls on LSP .....	16
3.3.1 Dominating Climatic Control at SOS and EOS.....	16
3.3.2 Shift in Climatic Controls at SOS and EOS.....	17

4	Discussion .....	20
4.1	Comparing LAI <sub>re</sub> to LAI <sub>3g</sub> .....	20
4.1.1	Raw LAI Data.....	20
4.1.2	LSP Parameters .....	21
4.1.3	Trends in SOS, EOS and GSL (1982 – 2011).....	22
4.1.4	Limitations due to the dependence on MODIS LAI.....	22
4.2	Climatic Controls .....	23
4.2.1	Yearly Dominating Controls.....	23
4.2.2	Quarterly Trends for Climatic Controls.....	24
4.2.3	Limitations of the climatic control model (extended GSI).....	27
4.3	Influence of Climatic Controls on LSP .....	27
4.3.1	Dominating Controls at SOS and EOS.....	27
4.3.2	Start of Season in the Northern Hemisphere.....	28
4.3.3	Start of Season in the Southern Hemisphere .....	29
4.3.4	End of Season in the Northern Hemisphere .....	30
4.3.5	End of Season in the Southern Hemisphere.....	31
4.3.6	Limitations.....	31
5	Conclusion and Outlook .....	33
	References.....	35
	Acknowledgements .....	40
	Appendix A: Code used for processing.....	41
	Appendix B: Parameterization for HANTS-processing.....	42
	Personal Declaration .....	43

## List of Figures

<b>Figure 1:</b> Example of a discontinuous LAI profile near the equator in the LAIre dataset.	5
<b>Figure 2:</b> Illustration of the extraction methods for LSP parameters. The Midpoint (MP) method sets the date of $SOS_{MP}$ at half the total intra-annual peak-to-peak amplitude. The Maxincrease (MI) method sets the date of $SOS_{MI}$ at point of steepest increase in the LAI profile. EOS is set at the point where the curve goes under the SOS value again.	6
<b>Figure 3:</b> Flowchart showing processing chain from raw LAI datasets to final maps of dominating controls, shifts of climatic controls and SOS/EOS shifts used to discuss the influence of climatic controls on LSP.	9
<b>Figure 4:</b> SOS and EOS are extracted from LAI profile (black) and then climatic controls (red, blue, green, taken from Jolly et al., 2005) in the 30 days prior to SOS/EOS can be extracted.	10
<b>Figure 5:</b> Correlation coefficients between LAIre and LAI3g for each 15-day period from 1982 – 2011.	11
<b>Figure 6:</b> Difference in days for SOS (left) and EOS (right) estimations from LAIre relative to LAI3g for 1996, extracted with the midpoint method. Negative values (brown) represent an earlier date in LAIre than LAI3g, positive values (blue) represent a later date in LAIre than LAI3g.	12
<b>Figure 7:</b> Trends in in Growing Season Length from 1982 – 2011 for LAI3g (left) and LAIre (right) in days/decade.	13
<b>Figure 8:</b> Yearly dominating controls in 1982 (left) and 2010 (right) showing large-scale change in moisture control in Brazil.	14
<b>Figure 9:</b> Quarterly changes in temperature limitation.	15
<b>Figure 10:</b> Quarterly changes in moisture limitation.	15
<b>Figure 11:</b> Dominating controls at EOS for the years 1991 and 1992 showing big variability particularly for Europe and Northern America.	17

<b>Figure 12:</b> Shifts in moisture limitation at SOS and EOS from 1982 – 2011 based on LSP parameters extracted from LAIre.....	18
<b>Figure 13:</b> Shifts in temperature limitation at SOS and EOS from 1982 – 2011 based on SOS/EOS extracted from LAIre.....	18
<b>Figure 14:</b> Shifts in radiation limitation at SOS and EOS from 1982 – 2011 based on SOS/EOS extracted from LAIre.....	19
<b>Figure 15:</b> Scatterplot of raw values from LAI3g and LAIre for the period of September 1. – 15. 1985. Green: Differences due to resampling of LAI3g dataset (coastal areas). Red: Saturation effect of LAI3g in the tropics where LAIre estimates higher values. ....	20
<b>Figure 16:</b> Vulnerability of EOS-date extraction to small changes in LAI-value of SOS/EOS due to the gentler slope during senescence.....	21
<b>Figure 17:</b> Map showing the number of different dominating controls from 1982 – 2011. Areas with 2 dominating controls correspond to ecotones.....	23
<b>Figure 18:</b> Comparison of (a) dominating controls at SOS, (b) changes in the temperature limitation during the second quarter of the year and (c) decadal change of SOS from 1982 – 2011.....	28
<b>Figure 19:</b> Shift in temperature control (a) and LAI (b) for March to June for 1982 and 2011 towards an earlier date in the northern hemisphere.....	29
<b>Figure 20:</b> Comparison of (a) dominating controls at SOS, (b) changes in moisture limitation in the 3 <sup>rd</sup> quarter and (c) decadal change of SOS from 1982 – 2011 for South America and Africa.....	29

## List of Tables

<b>Table 1:</b> Average Pearson’s correlation coefficients and covariance of bimonthly raw and yearly mean, minimum and maximum LAI values.....	11
<b>Table 2:</b> Average Pearson’s correlation coefficients comparing LSP parameters extracted from LAIre and LAI3g with the Midpoint (MP) and Maxincrease (MI) method.....	12

# 1 Introduction

The effects of anthropogenic climate change on vegetation dynamics have received increasing attention from the scientific community in the past decades (Schwartz 1999; Richardson et al. 2013). As part of this, global and regional changes in the regional and global seasonality of vegetated land surfaces, so called Land Surface Phenology (LSP), have been documented (de Jong et al. 2012; Garonna et al. 2014; Jeong et al. 2011; Anwar et al. 2015; Badeck et al. 2004; Julien & Sobrino 2009). The feedback loops of phenology and the climate system have to be investigated to understand the processes underlying these changes in LSP and to be able to make predictions for the future (Richardson et al. 2012; Richardson et al. 2013). Developing climate based LSP models and comparing them to the effects observed in satellite and field data are important steps to investigate these complex interactions (Schwartz 1999; Jolly et al. 2005). A promising concept to model phenology is based on climatic factors limiting plant growth, also called climatic controls (Jolly et al. 2005). Jolly et al. developed a Growing Season Index (GSI) based on three climatic factors: minimum temperature, vapour pressure deficit (VPD) as a measure of moisture availability and photoperiod to quantify light availability. The GSI uses thresholds and linear relationships to model the limitation the three climatic controls impose on plant growth (Jolly et al. 2005). Stöckli et al. (2011) have used and extended the GSI to perform a global reanalysis of vegetation phenology, creating global modelled time-series of Leaf Area Index (LAI). Most studies on long-term LSP trends are based on remotely sensed data (e.g. de Jong et al. 2011; Garonna et al. 2014; Jeong et al. 2011) and use the Normalized Difference Vegetation Index (NDVI) (Tucker 1979; Rouse et al. 1973). Since the NDVI is a one-dimensional proxy of vegetation activity based on the reflectance of visible and infrared radiation, its application for understanding the multi-dimensional system of underlying processes is limited (Myneni et al. 1995; Carlson & Ripley 1997; Jiang et al. 2006; Jin & Eklundh 2014). The NDVI does not provide a direct link to biophysical parameters and is therefore not very suitable to model or to compare to field data, which is why the LAI is increasingly considered a more reliable indicator of leaf-state from remotely sensed data. The LAI can also be derived from remotely sensed data, and contrary to the NDVI, the LAI allows a direct link to ground conditions (Zhu et al. 2013; Jiang et al. 2010). Satellite based LAI products have been available from the Moderate Resolution Imaging Spectroradiometer (MODIS) and SPOT/VEGETATION (Baret et al. 2007) platforms since 2000 (Fang et al. 2012) and have been used for short-term LSP studies (Verger et al. 2015; Anderson et al. 2015). Longer LAI time-series have recently been developed by

linking 30 years of Advanced Very High Resolution Radiometer (AVHRR) NDVI data to the available MODIS LAI data (Zhu et al. 2013).

With the emergence of long-term LAI time-series, it has become possible to compare modelled LAI datasets such as the reanalysis done by Stöckli et al. (2011) to measured datasets from remotely sensed data. This gives us a chance to verify the models and it allows us to study the potential impact of the climatic controls over the past 30 years. Of particular interest to LSP researchers are parameters indicating the start of spring events called Start Of Season (SOS) and senescence, usually called End of Season (EOS) (Reed et al. 2003). Quantifying and understanding the changes in climatic controls over the past decades during these events is an important effort in our quest to understand the interactions between LSP and changes in the atmosphere (Jeong et al. 2011; Richardson et al. 2013).

Given this context, this master thesis focuses on the impact of global changes in climatic controls on global LSP. The thesis is structured in three parts, each addressing a particular research question. Firstly, the modelled LAI is compared to the measured LAI to validate the climatic controls model. Of major interest for validation are LSP parameters SOS and EOS extracted from the two dataset. The validation will justify the use of the climatic controls model to explain changes in LSP. To understand where changes in climatic controls might not be the main drivers of LSP, differences between modelled and measured data will be investigated. Therefore, the main question answered in this first part is: How well do LSP parameters (such as SOS and EOS) extracted from the two datasets correlate and where do they differ?

Secondly, the three climatic controls on which the modelled LAI is based (minimum temperature, VPD and radiation) are examined to gain an understanding of the changes in global climatic limitations for plant growth. Inter-annual changes in dominating controls are investigated as well as changes in the strength of individual controls over the last 3 decades. This is used to answer the question: Are there changes in dominating climatic controls or in individual controls over the last 30 years?

Lastly, climatic controls at the time of SOS and EOS and their changes over the last 30 years are analysed to gain an understanding of the processes influencing these important phenological stages. Changes in the controls influencing SOS and EOS will be examined to answer the question: Are there inter-annual changes in global dominating or individual climatic controls at SOS and EOS?

## 2 Data & Methods

### 2.1 Leaf Area Index datasets

The Leaf Area Index is defined as half of the green leaf area relative to the ground area, usually with values ranging between 0 and about 8 m<sup>2</sup>/m<sup>2</sup> (Chen & Black 1992; Fernandes et al. 2014). Two LAI datasets have been used in this thesis, a modelled dataset (LAIre) and a remotely sensed dataset (LAI3g). The modelled LAIre comes from the global reanalysis of vegetation phenology (Stöckli et al. 2011), the measured LAI3g is based on the longest available global NDVI time-series from the Global Inventory Monitoring and Modelling Systems (GIMMS) group, the AVHRR NDVI3g (Tucker et al. 2005; Pinzon & Tucker 2014). The data were processed over a period of 30 years (1982 to 2011).

#### 2.1.1 LAIre – Modelled LAI

Stöckli et al. (2011) developed a global LAI dataset with a model based on Jolly's (2005) climatic controls used in the Growing Season Index (GSI). Jolly used two thresholds for each control: a minimum threshold where growth is fully limited, and maximum threshold where plant growth is not limited anymore. In between the minimum and maximum threshold, a linear gradient is assumed. For temperature and photoperiod this gradient ranges from 0 at the minimum threshold to 1 at the maximum threshold. The scale for VPD is inverted because a higher vapour pressure deficit results in less available moisture. They used European Centre for Medium-Range Weather Forecast (ECMWF) ERA-Interim data to calculate daily climatic controls.

Stöckli et al. extended the GSI model into a prognostic phenology model to predict LAI and Fractional Photosynthetically Active Radiation (FPAR). They included a set of 35 natural and non-natural plant functional types (PFT) to more accurately represent different vegetation types and other land-cover types such as urban areas or water bodies, and set different thresholds for each PFT, based on prior research. The percentage of each PFT for each pixel is set based on a combination of several MODIS land-cover, vegetation and crop products and is kept static over the years. Finally, MODIS LAI and FPAR data from 2000 to 2009 were used to assimilate the model to actual LAI and FPAR values.

The final LAIre dataset provides daily LAI and FPAR estimates for the past 50 years with a global ½ degree spatial resolution. In addition to the modelled LAI values the dataset

also includes daily climatic control factors for temperature, VPD and radiation, on which the model is based.

### *2.1.2 LAI3g – Measured LAI*

The remotely sensed LAI dataset was derived from the third generation GIMMS AVHRR NDVI dataset (NDVI3g) (Zhu et al. 2013; Pinzon & Tucker 2014). They used temporally overlapping MODIS LAI data from 2000 to 2009 to train a neural network with the NDVI3g. The resulting LAI3g is a dataset with a global  $1/12$ -degree spatial resolution and a 15-day (bimonthly) temporal resolution for the years 1982 to 2011.

It is important to note that the 15-day temporal resolution of the NDVI3g, and therefore also the LAI3g, is based on an unknown number of actual acquisitions within each 15-day period. Due to the processing of the NDVI to create the NDVI3g, it is not possible to extract the exact date of each acquisition in order to assess cloud cover or other influencing factors (Pinzon & Tucker 2014).

## 2.2 Methods

In this section, data pre-processing and the extraction of LSP parameters are described first, since these form the basis for answering all three research questions. Then, the methodology used to answer the three research questions is described. The data was processed using IDL for temporal and spatial resizing and smoothing of the data, and R was used for the extraction of LSP parameters and all the statistical analyses. An overview of the files used for processing can be found in Appendix A.

### *2.2.1 Data Pre-processing*

Both datasets were resampled to the same temporal and spatial resolution in order to be comparable. The temporal resolution of the LAIre was resized from daily to bimonthly using 15-day means to match the LAI3g dataset. The LAI3g dataset was resized spatially from  $1/12$ -degree to  $1/2$ -degree using bilinear resampling in a 6 x 6 window. If more than 50% of the pixels within the 6x6 window had no value, the pixel was excluded. If less than 50% of the pixels had no value, the no-value pixels were set to a LAI of 0 and included in the bilinear resampling. This was done to mimic the LAIre production, which similarly calculates the effect of water or desert-bodies based on the PFT percentage in the pixel.

Due to the half-year shift in growing seasons between the Northern and Southern Hemisphere, both datasets were split by hemisphere. The Southern Hemisphere was redefined to start in the middle of each year (scene 13 out of 24 bimonthly scenes) and last until the middle of the following year (scene 12 of the following year). Since there

was no data for the year 2012 which could be added to the year 2011 in the Southern Hemisphere, the first 12 scenes of 2011 were added as a substitute to get a complete growing season.

### 2.2.2 Extraction of Land Surface Phenological Parameters

LSP extraction is usually done by first smoothing the dataset to eliminate artifacts from cloudy or dead pixels and by then extracting a Start Of Season (SOS), End Of Season (EOS) and Growing Season Length (GSL) for each year (Garonna et al. 2014; de Jong et al. 2011).

#### *Smoothing the dataset*

The smoothing of the dataset was done using the Harmonic Analysis of NDVI Time-series (HANTS) algorithm (Roerink et al. 2000; Roerink et al. 2003). The algorithm applies a Fast Fourier Transform (FFT) to the measured values and extracts first, second and third order sine-functions to produce a smoothed version of the original signal. Even though the algorithm was originally developed for NDVI time-series, it can be used for LAI datasets in the same way (Jiang et al. 2010). A more detailed description of the HANTS algorithm and the exact parameterization used for the extraction can be found in Appendix B.

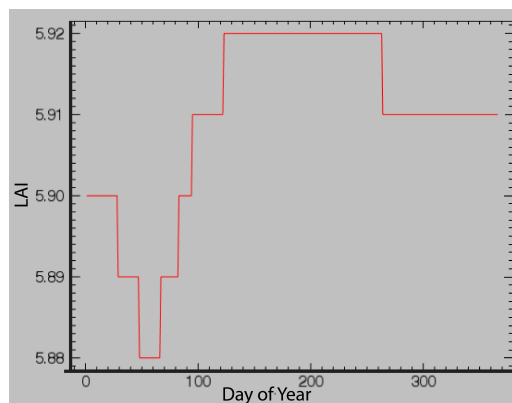


**Fig. 1:** Example of a discontinuous LAI profile near the equator in the LAIre dataset.

The LAIre does not suffer from cloud-contamination, and therefore produces generally much smoother profiles than the raw LAI3g data. The data were still processed with HANTS, to ensure that no differences due to differing processing chains were introduced. Additionally, the LAIre suffers from non-continuous LAI profiles for some pixels particularly in the tropics (Fig. 1), which are conveniently eliminated by applying HANTS.

#### *LSP Parameters*

A variety of methods exists to define the SOS (Reed et al. 2003), with no clear agreement on a single metric or definition. However, the Midpoint (MP) and Maxincrease (MI) methods (Fig. 2) have been put forward as being more closely related to ground phenological events in a large inter-comparison study (White et al. 2009) and have therefore been selected for this thesis. The Midpoint method defines SOS as the value

halfway between lowest and highest LAI value within one year. The Maxincrease method defines SOS at the point where the LAI curve shows the steepest positive slope – or in other words, where the first derivative of the curve is maximal. The EOS is usually defined as the date after SOS on the LAI curve where the LAI drops below the SOS value again. The Growing Season Length (GSL) is then just the difference between End and Start of Season expressed in days.

### *Implementation of LSP parameter extraction*

Since the extraction of LSP parameters is a fundamental concept of most research in remote sensing of LSP, it warrants a closer look in this thesis.

First, water bodies were masked out and pixels that show a weak intra-annual LAI variability below a threshold of 0.5 were filtered out. This was done mainly in desert areas where no vegetation is present and in tropical areas where vegetation shows no clear seasonality and the LAI remains high all-year long.

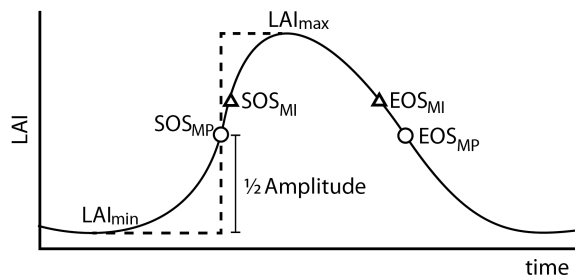


**Fig. 2:** Illustration of the extraction methods for LSP parameters. The Midpoint (MP) method sets the date of  $SOS_{MP}$  at half the total intra-annual peak-to-peak amplitude. The Maxincrease (MI) method sets the date of  $SOS_{MI}$  at point of steepest increase in the LAI profile. EOS is set at the point where the curve goes under the SOS value again.

The Midpoint method uses minimum and maximum LAI for each pixel and year and is calculated with  $LAI_{MP} = \frac{(LAI_{min} + LAI_{max})}{2}$ .

Then, the point in time where the LAI-curve first exceeds  $LAI_{MP}$  is defined as the SOS (Fig. 2).

The implementation of the Maxincrease method is more challenging in its conception since the theoretical definition is based on continuous data rather than the discrete data points that are being

processed in practice. In this thesis, an algorithm described in Garonna et al. (2014, 2015 submitted) was used. This algorithm also uses a more thorough filtering method for pixels where an extraction is not possible, by flagging pixels showing more than one growing season within a year as well as growing seasons straddling the year end (Garonna et al. 2014).

To understand the mechanisms of LSP parameter extraction, an attempt was made at implementing the MP and MI extraction methods, rather than relying on already available algorithms. While the Midpoint method was implemented as described here, the implementation of the MI method followed a simplified approach based on the

assumption that the maximum increase must occur between the two adjacent data points ( $LAI_i$  and  $LAI_{i+1}$ , which have the highest positive difference in LAI between them). The  $LAI_{MI}$  can then be defined as  $LAI_{MI} = \frac{(LAI_i + LAI_{i+1})}{2}$ . Then the extraction follows as for the Midpoint method.

Even though the MP method showed very similar results as the algorithm used by Garonna et al., the Maxincrease methods showed a bigger variability of the data due to the two different approaches used. To make the results more comparable to other similar studies with NDVI3g and LAI3g datasets (Garonna et al. 2014, Garonna et al., submitted), it was decided to use the more advanced algorithm for further processing.

### 2.2.3 Comparing LAI<sub>re</sub> to LAI<sub>3g</sub>

#### *Raw LAI values*

To make a first assessment on the comparability of the two datasets, the raw values for each 15-day period were correlated for every year. Pearson's r was used for the correlation statistics, because a linear 1:1 relationship is the expected in the ideal case. Correlation statistics and scatterplots were also calculated for yearly mean, minimum and maximum values for each pixel to check for any systematic over- or underestimations in the modelled or the measured dataset.

#### *Comparing Phenological Parameters*

A linear regression was performed to compare the extracted LSP parameters SOS, EOS and GSL from the two datasets for both MP- and MI-extracted parameters. A separate linear regression was performed for the region between 45 degrees and 90 degrees northern latitude to exclude effects from multiple annual growing seasons in the tropics and the Mediterranean zone. Maps showing the absolute difference in days between the parameters extracted from the two datasets were also computed. This allows for a more intuitive comparison on regional agreements and disagreements between the two datasets.

#### *Trends in SOS, EOS and GSL*

To complete the comparison of the two datasets, a linear trend analysis was conducted for all three extracted LSP parameters, the SOS, EOS and GSL, for the period 1982–2012. The rate of change of the three LSP parameters was expressed in days/decade for each pixel, following Garonna et al. (2014). To get this rate of change, a linear regression model was applied and the slope of the resulting linear fit taken. Pixels that did not show a significant change according to the Analysis Of Variance (ANOVA) with a significance level of  $\alpha = 0.05$  were discarded. If LSP parameters for more than 1/3 of all

years (i.e. more than 10 years of data) or either the first or last year could not be extracted, the pixel was also discarded. For pixels with less than 10 years of data missing, the missing LSP parameter-values were linearly interpolated. This was done to minimize effects of short-term changes in trends, which might otherwise skew the results if a significant part of observation was linearly interpolated rather than actually observed.

#### *2.2.4 Trends in Climatic Controls*

The yearly dominating climatic control for each pixel was extracted based on the GSI to investigate changes in dominant controls. For every pixel, the magnitude of each daily climatic control factor was integrated over the whole year. The climatic control with the lowest total sum was then chosen as the most limiting factor for each year. It is a simplified version of the approach described in Jolly et al. (2005) but was found to produce comparable results. This method does not adequately represent areas where two climatic controls are almost equally dominating in their limitation, however, when examined in a time series, those areas are easily identified since the two dominating controls both tend to show up alternating between years. To identify those areas more easily, the maps were analysed on changes per pixel over the 30 years. Pixels were then grouped into 3 classes: those that only have 1 dominating control over all years, those changing only between two specific climatic factors and those showing changes between all 3 climatic factors over the observed time period.

To show inter-annual changes in climatic controls for different times of the year, bimonthly means of each climatic control were extracted for each year. Then a linear trend analysis was performed for 15-day period similar to the decadal change method used in the LSP trend-analysis before. Instead of days per decade for LSP parameters, the climatic controls change is then expressed in percentage-points per decade. Finally, 6 bimonthly scenes each were aggregated to quarterly scenes to allow for a more intuitive interpretation of seasonal effects.

### 2.2.5 Influence of Climatic Controls on Land Surface Phenology

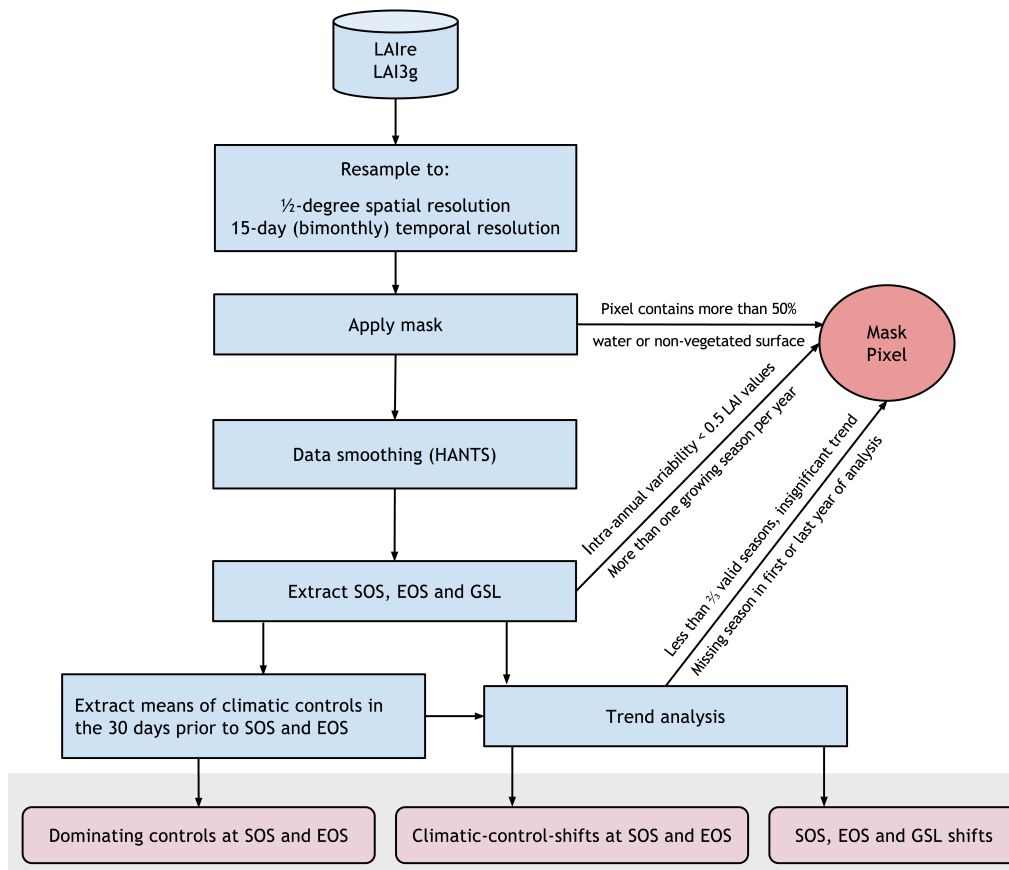


**Fig 3:** Flowchart showing processing chain from raw LAI datasets to final maps of dominating controls, shifts of climatic controls at SOS/EOS and SOS/EOS shifts used to discuss the influence of climatic controls on LSP.

To assess the effect climatic controls might have on SOS and EOS timing, mean values for each climatic control were extracted for the 30 days prior to SOS and EOS (see Fig. 4). 30 days was chosen as a time frame since it corresponds to the temporal uncertainty caused by the bimonthly resolution of the LAI3g. The extraction of climatic controls was done for LSP parameters extracted from both the LAI3g and LAIre dataset. Only the LSP parameters extracted with the MP method were used, because the shift of LSP parameters extracted from MI and MP methods are very similar, so a distinction between the two is not expected to produce significantly different results. Additionally, the MP method has proven to give more stable results and is therefore more useful for this trend-analysis of climatic controls by being less sensitive to outliers (Garonna et al. 2014).

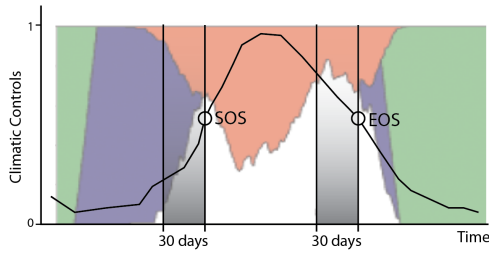


**Fig. 4:** SOS and EOS are extracted from LAI profile (black) and then climatic controls (red, blue, green, taken from Jolly et al., 2005) in the 30 days prior to SOS/EOS can be extracted.

With the extracted 30-day climatic control means, the dominating factors for each year were computed for both the 30-day period before SOS and before EOS, analogous to the methods described in section 2.2.3. These factors were used to study dominant factors during SOS and EOS as well as to study the effects of changes in climatic controls extracted in section

2.2.3 on the changes in LSP extracted in section 2.2.1.

A linear trend for the individual changes in climatic controls in the 30-day window prior to SOS and EOS was also computed and tested for significance on the  $\alpha = 10\%$  level.

This significance level was chosen because linear trends depend on shifts of SOS/EOS date as well as shifts in climatic controls. The resulting greater inter-annual variability leads to statistically lower significance levels.

### 3 Results

#### 3.1 Comparing LAIre to LAI3g

##### 3.1.1 Raw LAI Data

Correlating mean bimonthly LAI values resulted in an average Pearson's correlation

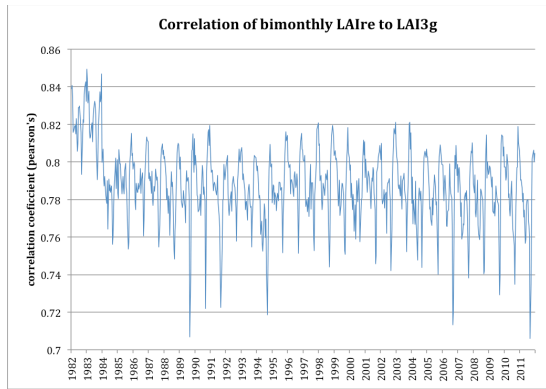


**Fig. 5:** Correlation coefficients between LAIre and LAI3g for each 15-day period from 1982 – 2011.

coefficient of  $r = 0.78$  with a standard deviation of 0.02. There is a clear break between December 1983 and January 1984 (see Fig. 5). The average correlation coefficient from 1982 to 1983 is  $r = 0.82$  whereas the period from 1984 to 2011 is at the total average of  $r = 0.78$ . The correlations showed periodical minima in the first half of September in all years,

deviating up to 0.08 from the average.

**Table 1:** Average Pearson's correlation coefficients and covariance of bimonthly raw and yearly mean, minimum and maximum LAI values.

	Average Pearson's R	Average covariance
bimonthly raw values	0.79	1.28
yearly means	0.90	1.23
yearly minima	0.84	0.75
yearly maxima	0.89	1.82

Yearly maxima showed an average correlation coefficient of  $r = 0.89$  and an average covariance of 1.82. Yearly minima showed an average correlation of  $r = 0.84$  and an average covariance of 0.74 and

yearly means show an average correlation of  $r = 0.90$  and an average covariance of 1.23. Scatterplots of yearly mean and minimum LAI values showed a distinct outlier group where LAIre pixels have a higher value than the corresponding LAI3g pixels (see Fig. 15).

##### 3.1.2 LSP Parameters

The LSP parameter extraction for the LAI3g was successful for 67% of land pixels on average per year. The other pixels were excluded due to a weak intra-annual variability or missing data. For the LAIre, 91% of all land-pixels were successfully processed. There were no significant differences in number of pixels extracted between the MI and MP

extraction methods. The annual correlation coefficients for the LSP parameters extracted with the MP method were on average around  $r = 0.30$  for SOS,  $r = 0.49$  for EOS and  $r = 0.56$  for the GSL globally. Correlation coefficients from the MI method averaged  $r = 0.26$  for SOS,  $r = 0.40$  for EOS and  $r = 0.43$  for GSL (Table 2).

**Table 2:** Average Pearson’s correlation coefficients comparing LSP parameters extracted from LAIre and LAI3g with the Midpoint (MP) and Maxincrease (MI) method.

		Global	Northern Hemisphere	Southern Hemisphere	45–90 deg. northern latitude
MP	SOS	0.30	0.40	0.23	0.72
	EOS	0.49	0.51	0.28	0.05
	GSL	0.56	0.58	0.37	0.38
MI	SOS	0.26	0.36	0.17	0.64
	EOS	0.40	0.45	0.18	0.09
	GSL	0.43	0.46	0.23	0.38

The lowest differences in SOS between LAIre and LAI3g were found for the regions with only one distinct growing season per year, such as the high northern latitudes with differences below 15 days for both extraction methods (Fig. 6). This also showed in the correlation coefficients for the latitudes 45 to 90 degree north, with an average correlation coefficient of  $r = 0.72$  for the MP method and  $r = 0.64$  for the MI method. Only a few regions in the Northern Hemisphere showed a later date for SOS for the LAIre of up to 60 days with the exception of India and East Asia where the LAIre showed an earlier SOS compared to the LAI3g. South of the tropics, the differences were more pronounced than in the Northern Hemisphere with differences in SOS of up to 60 days. In the tropics, differences above 120 days were found. Because much of the landmass of the Southern Hemisphere is tropical, the correlation coefficients were around  $r = 0.2$

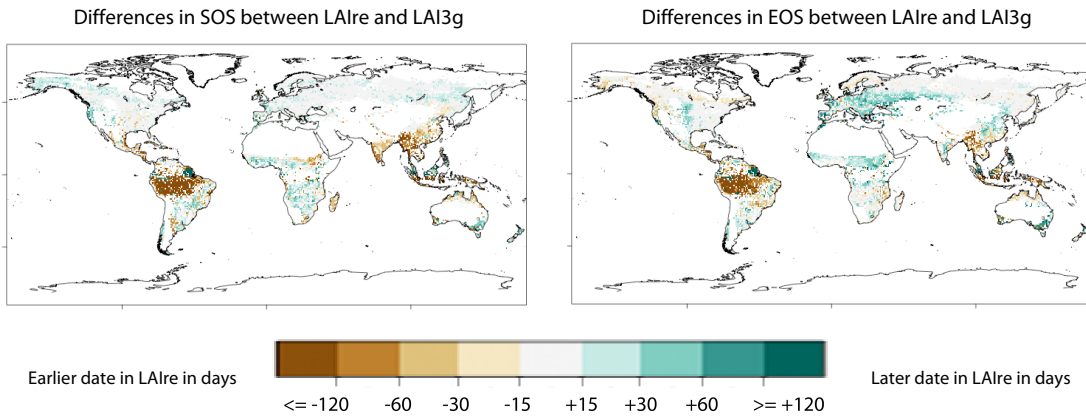


**Fig. 6:** Difference in days for SOS (left) and EOS (right) estimations from LAIre relative to LAI3g for 1996, extracted with the midpoint method. Negative values (brown) represent an earlier date in LAIre than LAI3g, positive values (blue) represent a later date in LAIre than LAI3g.

for both the MI and MP method for all 30 years with the sole exception of the GSL extracted from the MP method, where the two datasets correlate with  $r = 0.37$ . The EOS showed a much higher global variability between LAIre and LAI3g, with parts of Eastern Europe and central Asia where the LAIre showed both earlier and later dates for EOS of up to 60 days compared to the EOS from the LAI3g. The high variability resulted in correlation coefficients close to zero for the high northern latitudes between the two datasets. The same was found for parts south of the Sahara in Africa and eastern Asia, albeit less pronounced, where correlation coefficients were below  $r = 0.3$  for every year and for both extraction methods.

The differences in GSL were up to 60 days longer for the LAIre in the Northern Hemisphere, particularly in eastern Europe where the GSL was up to 120 days longer than in the LAI3g. The northernmost parts of Eurasia and America however showed a shorter GSL for the LAIre of up to 60 days for some years. In the Southern Hemisphere more variation was found with no clear large-scale over- or underestimations.

### 3.1.3 Trends in SOS and EOS (1982 – 2011)

A shift towards an earlier onset of the growing season for northern Europe and a later onset in southern America was seen in both datasets. The LAIre also showed a shift towards a later onset of SOS south of the Sahara where the LAI3g lacks data. A trend towards an earlier SOS was observed in China in the LAI3g, which was much less pronounced in the LAIre.

For GSL, South America as well as in the east of southern Africa showed a shortening in both datasets and a lengthening of GSL in northern Europe and China as well as in the west of southern Africa. Differing results were found south of the Sahara with the LAI3g indicating a slight GSL lengthening and the LAIre showing a shortening (see Fig. 7).

A trend of a later EOS was observed for southern Africa as well as in southern America

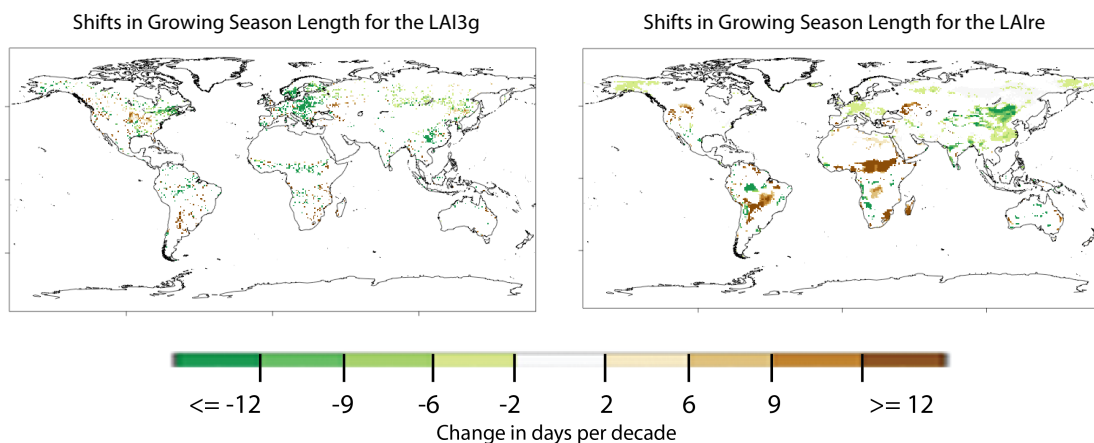


**Fig. 7:** Trends in in Growing Season Length from 1982 – 2011 for LAI3g (left) and LAIre (right) in days/decade. Differences are visible particularly in the Sahel.

in both datasets. The LAI3g showed a later EOS for northern Europe, which is not visible in the LAIre dataset. The LAIre however indicated a trend towards an earlier EOS for Central Asia, which is not visible in the LAI3g dataset due to lack of data.

## 3.2 Climatic Controls

### 3.2.1 Yearly Dominating Control

Temperature was found to be the dominating yearly control factor for the higher latitudes of the Northern Hemisphere. Radiation was shown to be the main control factor for the eastern USA, Europe and East Asia. Moisture was found to be the dominating control for the Middle East and most of Africa as well as most of Australia. The tropics were controlled by radiation, as is most of South America over all years in the observation period.

Changes in the dominating yearly control factor over 30 years were mainly found along the borders of areas of different dominating controls (see Fig. 8 and Fig. 17). Exceptions to this small-scale variability were South America and Scandinavia. Large regions in Brazil showed a clear shift in domination from radiation to moisture between 1982 and 2011 (Fig. 8). Scandinavia showed large-scale inter-annual variations of dominating controls, changing between radiation- and temperature-dominated years. A domination change between all 3 controls was only found in Central Asia, where areas of all three domination controls meet.

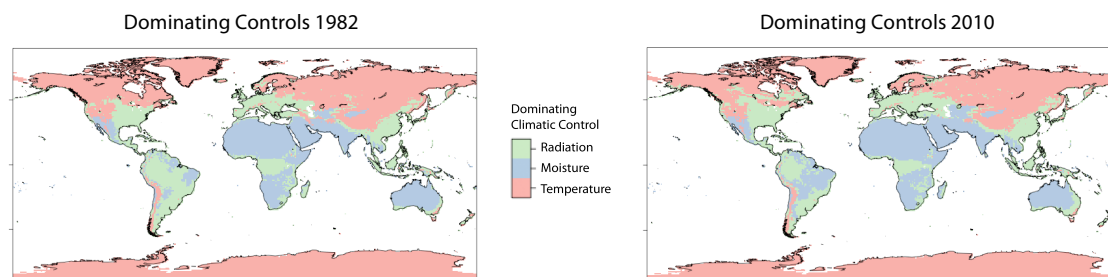


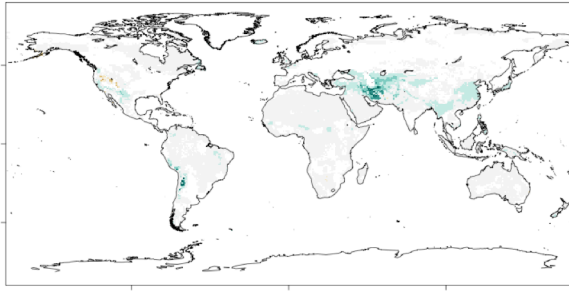
**Fig. 8:** Yearly dominating controls in 1982 (left) and 2010 (right) showing large-scale change in moisture control in Brazil.

### 3.2.2 Quarterly Trends for Climatic Controls

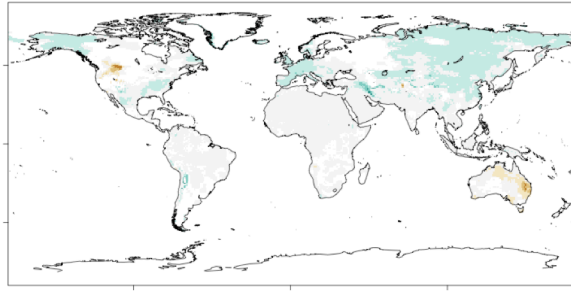
#### *Temperature*

A strong decrease of temperature control was observed in the first quarter of the year for the Middle East and central Asia with decadal change of over 20% in some parts (Fig. 9). The second quarter showed a decrease of temperature control in the northern latitudes, particularly Greenland and north-eastern Siberia with changes of 15% to 20% per decade. For the third quarter, the same decrease can be observed for the high latitudes of northern America. In fourth quarter of the year, a decrease in temperature

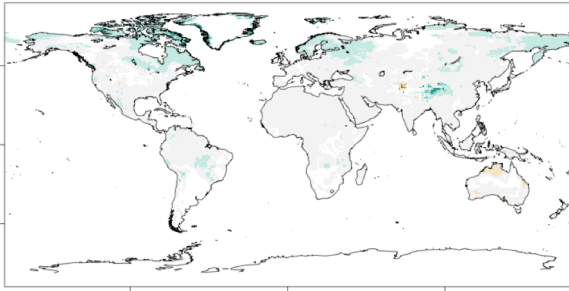
Decadal Change in Temperature Limitation: Q1



Decadal Change in Temperature Limitation: Q2



Decadal Change in Temperature Limitation: Q3



Decadal Change in Temperature Limitation: Q4

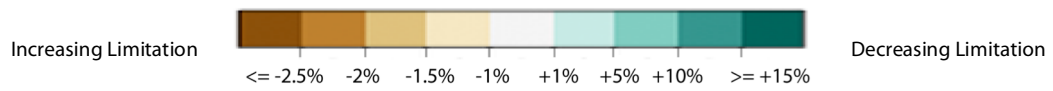
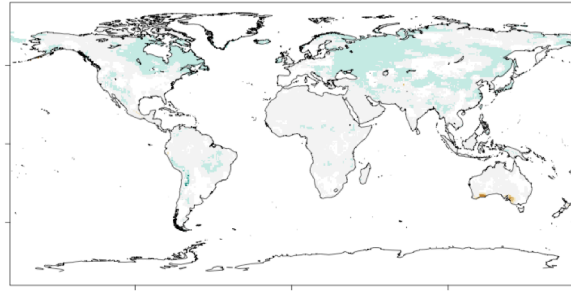
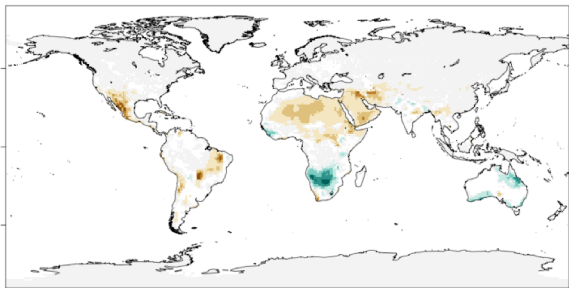
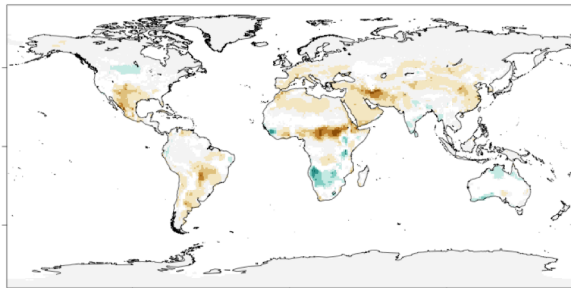


**Fig. 9:** Quarterly changes in temperature limitation in percentage points per decade.

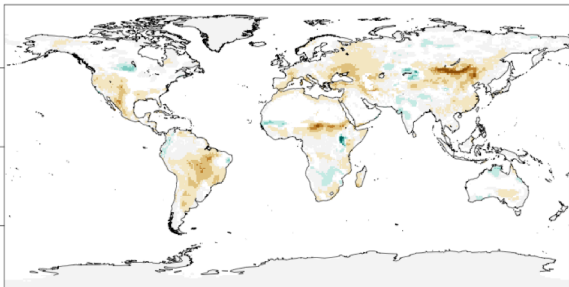
Decadal Change in Moisture Limitation: Q1



Decadal Change in Moisture Limitation: Q2



Decadal Change in Moisture Limitation: Q3



Decadal Change in Moisture Limitation: Q4

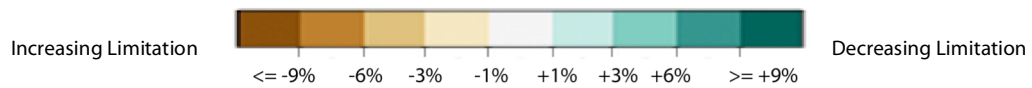
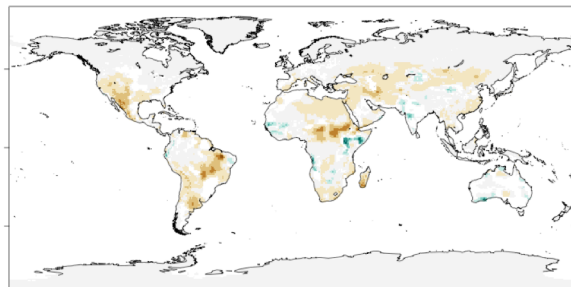


**Fig. 10:** Quarterly changes in moisture limitation in percentage points per decade.

control factor of 10% was found in Eastern Europe. An increase in temperature control was found in eastern Australia and South-western Canada during the second quarter of the year, where an increase in control of 2.5% per decade was observed.

#### *Moisture*

The moisture control showed a decrease of about 10% per decade for southern Africa in the first quarter of the year. Starting around March until May, the Middle East and the Sahel experienced an increase in moisture control of around 10% per decade. An increase in moisture control for the Gobi desert of over 10% was also observed in the second quarter of the year. The third and fourth quarter showed an increase in control for South America, mainly in Brazil, of over 10% per decade. Also in the fourth quarter an increase in control of over 10% for the south-eastern edge of the Sahara was found (Fig. 10).

### 3.3 Influence of Climatic Controls on LSP

The climatic controls at SOS and EOS showed similar results for LSP parameters extracted from either dataset. The main differences were found in the exact spatial extent and intensity of observed shifts, but they did not affect the general trends that were found. Therefore, the results presented here apply to both datasets, except when explicitly stated otherwise.

#### *3.3.1 Dominating Climatic Control at SOS and EOS*

##### *Dominating controls at Start of Season*

At the SOS date, the dominating control for the Northern Hemisphere was mainly temperature for higher latitudes in both hemispheres and radiation for lower latitudes. Moisture was the dominating limiting factor in the subtropics and radiation in the tropics. In the Southern Hemisphere the main limiting factor was moisture in the subtropics and radiation in the south of Africa, south of Australia and some parts of southern America. Only small parts of southwest America and south-eastern Australia were affected by temperature controls.

The time-series of dominating controls at SOS showed that the areas unaffected by changes in dominating controls, apart from desert and high mountainous areas, were in Siberia and parts of Canada, where the dominating control was temperature over all 30 years. A lot of inter-annual variability was observed in Europe and central Asia where the dominant control varied between temperature and moisture control. The Southern Hemisphere showed small variations in the extent of moisture-controlled and radiation-controlled areas.

### *Dominating Controls at End of Season*

At the EOS date, the Northern Hemisphere was dominated by radiation for most parts of central and eastern Europe, eastern and southern Asia and the east of North America. Central Asia, the Middle East and the north of Africa were dominated by the moisture control during EOS, as was the western part of the USA. The temperature control only showed domination in very high northern latitudes. The Southern Hemisphere was also mostly radiation controlled at EOS with the exception of Australia and southern Africa, which were mainly moisture controlled.

The time-series over the last 30 years showed a lot of large-scale annual changes between all 3 controls for most of the higher northern latitudes. For the rest of the world, only small variations around the border regions of dominating controls were found, mainly between moisture and radiation controlled areas.

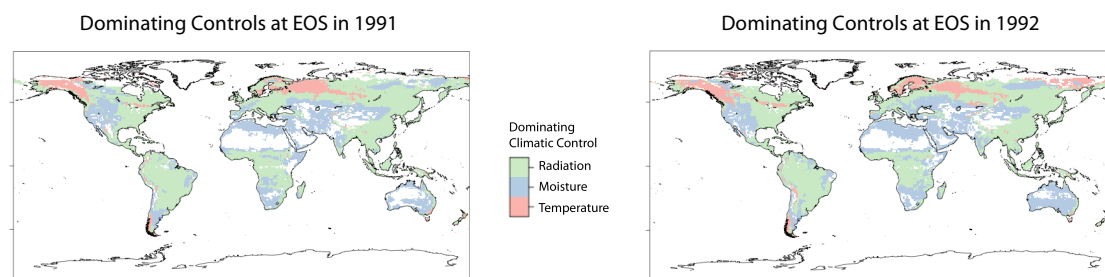


**Fig. 11:** Dominating controls at EOS for the years 1991 (left) and 1992 (right) showing big variability particularly for Europe and Northern America.

### *3.3.2 Shift in Climatic Controls at SOS and EOS*

#### *Moisture*

At the SOS date, a strong increase in influence of the moisture control of around 5% to 10% per decade was found in southern America, and in some areas even up to 14% per decade. A strong increase in control was also seen south of the Sahara with an increase of about 10% per decade. Western Africa, areas along the eastern Indian coast as well as northern East Asia showed a decrease in control, particularly in the LAIre dataset.

Almost no change in the influence of moisture control during the growing season for the Northern Hemisphere was found.

At the EOS date, an increase in moisture control for the Northern Hemisphere (1% – 5% per decade) and some areas in central and eastern Asia (over 13% per decade) was found. A slight increase in moisture control was also observed in southern America with a rate of about 3-9% per decade. Southern Africa and eastern Australia showed a decrease in moisture control of 10% per decade.

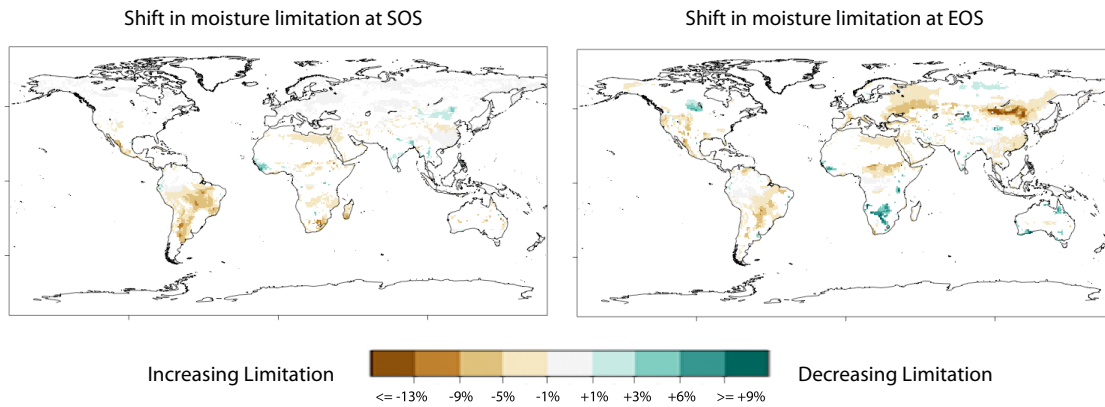


**Fig. 12:** Shifts in moisture limitation at SOS (left) and EOS (right) from 1982 – 2011 based on LSP parameters extracted from LAIre. Trends are given in percentage points per decade.

### *Temperature*

The temperature control showed a decline in influence at SOS of up to 15% per decade in Scandinavia, parts of central and eastern Asia as well as Brazil and southern Africa. An increase of temperature control was only observed around the Gobi desert (-13% per decade) and in north-eastern America (-5% per decade). At EOS a decline in temperature limitation was mainly be seen in the Northern Hemisphere with no significant major changes in the Southern Hemisphere.

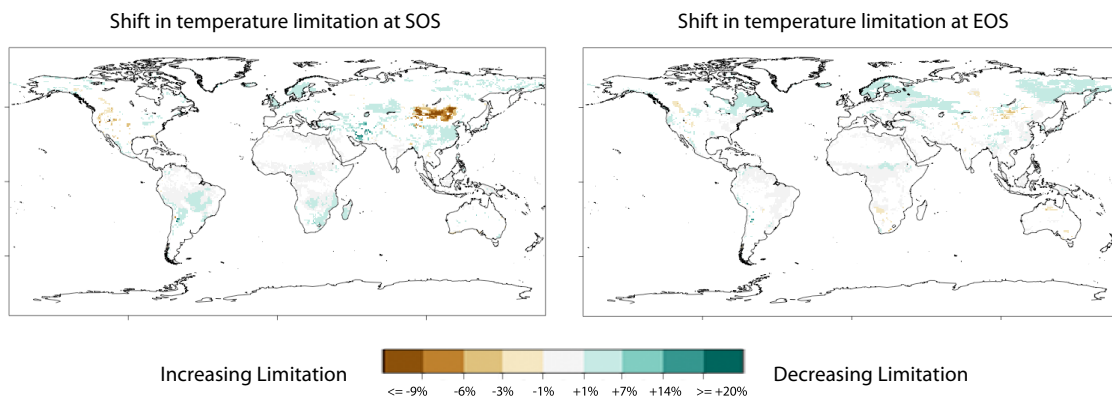


**Fig. 13:** Shifts in temperature limitation at SOS (left) and EOS (right) from 1982 – 2011 based on SOS/EOS extracted from LAIre. Trends are given in percentage points per decade.

### *Radiation*

In the Northern Hemisphere, radiation was found to become a stronger control at SOS with a rate of up to 10% per decade, except for parts of northern America where the effect is not as strong with only about 1-5% increase in control. Southern Africa showed a strong decrease in radiation control at SOS of about 10% per decade. A decrease at SOS was also observed in southern America where the increase is up to 8% per decade. Change rates during the EOS showed less agreement between the two datasets. The two regions where they agree were eastern Asia and southern Africa, where an increase of

radiation control at around 5% per decade was found at EOS. The LAI3g also showed an increase in radiation control of about 7% for many parts of North America, Europe as well as the Sahel, where the LAIre did not show any major change in control factor. A decrease of the radiation control of around 7% per decade in central Asia was found in the LAIre, however.

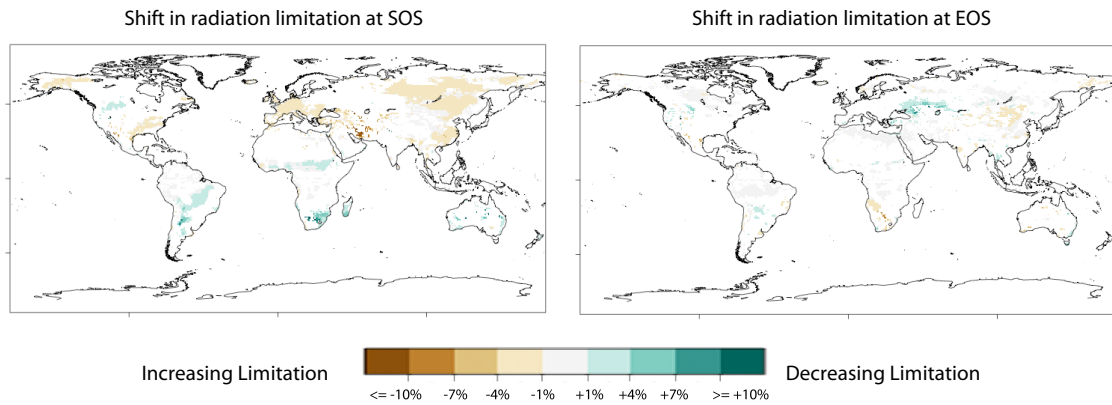


**Fig. 14:** Shifts in radiation limitation at SOS (left) and EOS (right) from 1982 – 2011 based on SOS/EOS extracted from LAIre. Trends are given in percentage points per decade.

## 4 Discussion

In this chapter, the methodology and results are interpreted to answer each of the three research questions. Then, a more general discussion of challenges and limitations of the methodology used in this thesis is presented.

### 4.1 Comparing LAIre to LAI3g

#### 4.1.1 Raw LAI Data

The high correlation coefficients between raw bimonthly LAIre and LAI3g data as well as mean, minima and maxima indicate that the model created by Stöckli et al. (2011) produces LAI values similar to remotely sensed data and that it can therefore be used for further analysis. Variations between the two datasets can be explained mainly by the pre-processing of the data. The spatial resampling of the LAI3g led to the biggest differences between the two datasets. These differences are concentrated in coastal areas due to mixed water and land pixels (see Fig. 15). A further uncertainty comes from the way the 15-day LAIre values were produced. A bimonthly value represents the mean of daily, modelled LAI values. In the LAI3g dataset on the other hand, a bimonthly value represents the mean of an unspecified number of acquisitions for each 15-day period. Furthermore, atmospheric effects and the saturation of values at higher LAI in densely vegetated areas can play a role, mainly in the LAI3g data (Zhao et al. 2012). This is particularly evident when looking at a scatterplot between two datasets (Fig. 15) where a group of pixels in the tropics show a bigger LAI in the LAIre dataset whereas the LAI3g shows a saturation effect and therefore lower LAI values.

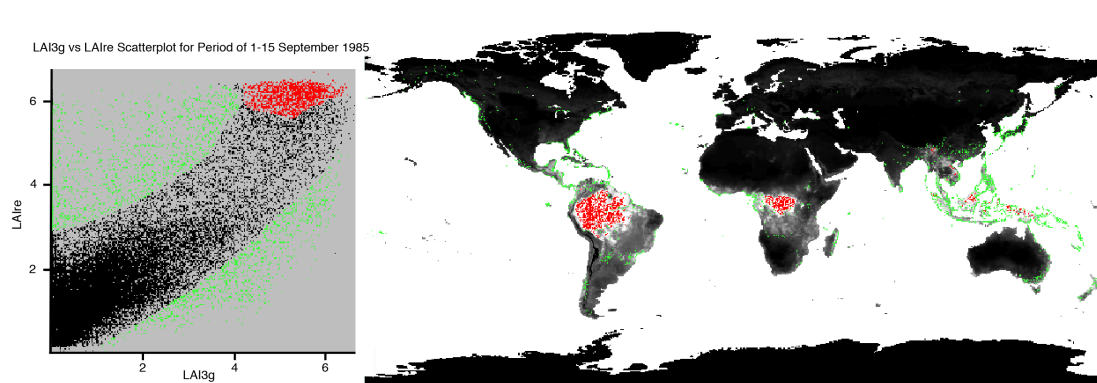


**Fig. 15:** Scatterplot of raw values from LAI3g and LAIre for the period of September 1. – 15. 1985. Green: Differences due to resampling of LAI3g dataset (coastal areas). Red: Saturation effect of LAI3g in the tropics where LAIre estimates higher values.

#### 4.1.2 LSP Parameters

The low correlation coefficients for all extracted LSP parameters globally (ranging between  $r = 0.26$  and  $r = 0.56$ ) might suggest that there is little agreement between the two datasets, but visual analysis of the geographical distribution refines this picture. The two datasets agree well in regions with one distinct growing season per year, for example in high and moderate northern latitudes. This shows in the high correlation coefficients (ranging from  $r = 0.64$  to  $r = 0.72$ ) for the SOS between 45 to 90 degrees northern latitude (Table 2). In those regions, differences of around 15 to 30 days remain and are inherent to the temporal resolution of the datasets of 15 days (Fig. 6).

The weaker correlation coefficients for EOS (ranging from  $r = 0.05$  to  $r = 0.49$ ) suggest that more complex factors are at play in autumn. The main factor leading to low correlation coefficients is that the LAIre does not show a clear trend towards over- or underestimating the EOS, but rather shows variability in both directions. There are some factors specific to the EOS that add to the variability and the bigger absolute differences observed. On one hand, climatic factors such as temperature have been shown to influence autumn phenology several months in advance of actual EOS (Jeong et al. 2011), which is not taken into account in the modelled LAIre. On the other hand, the

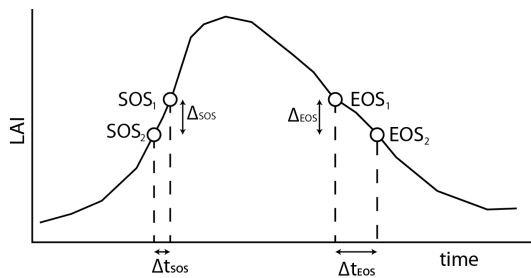


**Fig. 16:** Vulnerability of EOS-date extraction to small changes in LAI-value of SOS/EOS due to the gentler slope during senescence.

extraction of the EOS itself is subject to more variability than that of the SOS because the LAI profile usually has a steep slope during SOS, but a gentler slope during EOS. This makes the EOS-extraction more susceptible to

differences in extracting the date of EOS (see Fig. 16).

Tropical, subtropical and Mediterranean regions show more variability in extracted LSP parameters, which corresponds to prior findings (White et al. 2009; Garonna et al. 2014) and should therefore be used with caution when attempting to verify the modelled LAIre. Growing patterns and the LSP extraction methods mainly explain the differences in those regions. In tropical regions for example, where there is no clear start and end of season, small differences in data can lead to LSP shifts of half a year. Similarly, Mediterranean regions may show more than one distinct growing season, which can lead to differences in LSP parameter extraction.

The effect of different LSP extraction methods can also be seen when comparing the results from the MI method to the MP method. The correlation coefficients for the LSP

parameters extracted with the MI method are substantially lower compared to the MP method. This corresponds to prior findings where the MI method showed more variability from year to year compared to the more stable MP method (Garonna et al. 2014). This suggests that the MP method is more reliable for validation.

#### *4.1.3 Trends in SOS, EOS and GSL (1982 – 2011)*

The trend analysis for both dataset showed similar regional patterns for all three LSP parameters. The change rates were, however, stronger in the LAI3g dataset compared to the LAIre. This is particularly true for areas in China, where the LAI3g showed a strong shift in SOS towards an earlier day of the year, whereas the LAIre showed almost no change in those areas over the last 30 years. This difference in measured data and modelled data suggests that non-climatic factors might be responsible for the observed change. Improved agricultural productivity to support economic and population growth (Cao & Birchenall 2013) most likely caused these particular shifts. The LAIre model assumes static land-cover and therefore cannot reproduce LAI changes due to non-climatic drivers.

A difference in the two datasets was also found in the ecotone between savannah and desert in the Sahel. The big differences in GSL are due to different trends observed for SOS and EOS in the two datasets. The LAIre showed a later onset of SOS than the LAI3g, which leads to a shortening of the GSL in the LAIre data. The LAI3g however showed a trend towards slightly later onset of EOS, leading to an increase of the GSL. Satellite-based observations and corresponding field observations of increased vegetation activity in the Sahel in the last 30 years were already described by Dardel et al. (2014) and others (de Jong et al. 2011; Anyamba & Tucker 2005). The difference in modelled and remotely sensed observations most likely arises from re-greening of the Sahel in the past 30 years and therefore the changes in land-cover type (Foody 2001; Dardel et al. 2014; Mishra et al. 2015). The LAIre is unable to model these changes accurately due to the aforementioned static land-cover. This would suggest that dynamic land-cover estimations are needed to model the changes in ecotones, particularly along deserts where land-cover change is a prerequisite for changes in LSP.

#### *4.1.4 Limitations due to the dependence on MODIS LAI*

While the results from the comparison of the two LAI products suggest a generally good agreement of modelled data to remotely sensed data, it has to be considered that both the LAI3g and LAIre are connected to the Collection 5 Terra MODIS LAI product and therefore not completely independent from each other. In the case of the LAI3g, MODIS LAI from 2000 to 2009 was used to train the neural network algorithm to link NDVI3g

data to MODIS LAI data (Zhu et al. 2013). To produce the LAI<sub>re</sub>, MODIS LAI was used for data assimilation (Stöckli et al. 2011). A verification of the modelled LAI<sub>re</sub> with a MODIS-independent product such as the LAI CYCLOPES global product (Baret et al. 2007) would be desirable, once longer time series are available. For the time being, the LAI3g is, however, the only reliable long-term LAI dataset available and therefore more suitable for a verification of the modelled dataset.

Aside from the problem of interdependence of the two products, it is also worth looking at how well the products correspond to actual field data. Fang et al. (2012) compared both, MODIS and CYCLOPES LAI to in-field measurements. They found that while both products achieve good and very similar results, the uncertainties associated with both products are still outside of the requirements for “satellite based data products for climate”, as defined by the World Meteorological Organization (GCOS 2011). This is an important limitation at the moment since the LAI is viewed as a key measure to connect remotely sensed data directly to biophysical parameters (Fernandes et al. 2014).

## 4.2 Climatic Controls

### 4.2.1 Yearly Dominating Controls

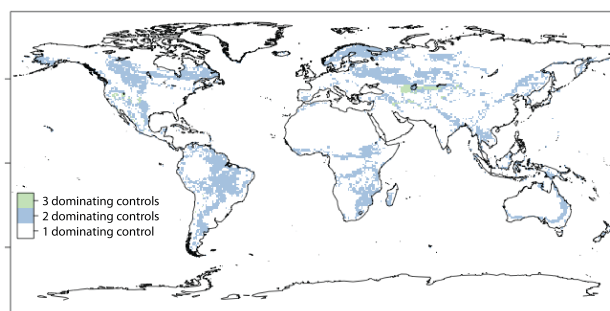


**Fig. 17:** Map showing the number of different dominating controls from 1982 – 2011. Areas showing 2 dominating controls correspond to ecotones.

the last 30 years. These areas show border areas of dominating controls. Interestingly, they also coincide with ecotones, the borders of different global ecosystems. This finding could potentially be used to study long-term changes in global ecotones by analysing changes in their spatial extent over time.

Visible and large-scale change of dominating control was observed in South America where parts of Brazil changed from a radiation-control dominated environment in the 1980s to a moisture-controlled environment in the 2000s. This change coincides with several strong drought events in Brazil in the years 2000 – 2010 (Anderson et al. 2015). Drought events are extreme weather phenomena, therefore the change in dominance

The results for yearly dominating controls mirror those of Jolly et al. (2005). In contrast to Jolly, no areas of “no seasonal constraints” in the tropics were defined, instead those areas appear as radiation controlled since photoperiod is the limiting factor. Fig. 17 shows the number of different dominating controls factors for each pixel over

should not be overstated yet, because changes in dominance are only visible from 2000 onwards. Further statistical analysis and longer time series are needed to assess long-term change in climatic controls in this region, independent of extreme events. Small changes in dominating controls run along borders of areas with different domination controls and vary by year without a clear trend in one direction. An interesting exception is northern Europe, which, even though it is temperature dominated in most years, showed some years (1989/1990, 2000 and 2005) where the radiation control became the dominating factor over a large area. A possible explanation of these outliers could be the North Atlantic Oscillation (NAO), which showed particularly positive NOA-index values for the affected years (Gouveia et al. 2008). However, interactions of ocean currents and LSP are very complex and further research is needed to find and confirm links between the two.

#### *4.2.2 Quarterly Trends for Climatic Controls*

To extend Jolly's (2005) analysis of how climatic controls vary within a single year, linear trends were extracted for each quarter of the year to give an insight into how the intra-annual controls change over the years. The radiation control will not be discussed in detail in this section since it showed no significant change over the last 30 years. This is due to the dependence on day-length, which has not changed considerably in the last 30 years.

##### *Temperature*

As expected based on the latest report from the IPCC (IPCC 2014), global rising temperatures led to a global decrease of influence for the temperature control factor. Changes in temperature controls were most visible in the Northern hemisphere, because the Northern Hemisphere was most affected by a dominating temperature control. A south-to-north pattern was observed starting in the Middle East in the first quarter and moving north towards northern Europe in the third quarter of the year. This stratified change in temperature control happens because the control factor only changes when temperatures are within the minimum temperature thresholds of the GSI-factor where growth is limited (around -2 to 5 degrees centigrade, depending on PFT) (Jolly et al. 2005, Stöckli et al. 2011). If temperatures change outside of this window of constraint, it will not be visible when looking at trends of climatic controls. Therefore, the change of temperature control coincides more or less with the 0-degree-centigrade line as it travels north in spring.

The highest rate of decreasing control of over 20% per decade was found in Iran in the first quarter. This strong change implies a clear change in growth limiting factors in the

next decade. This is particularly interesting because other studies found no significant mean, minimum and maximum temperature change for the first quarter of the year from 1960 to 2010 (Ghasemi 2015; Saboohi et al. 2012). Ghasemi (2015) mentions though that a steeper increase starting from the 1990s is expected. It has yet to be proven however if the change observed here is due to Ghasemi's expected change, if it is an artifact of the ERA-Interim dataset, or if it is a result of severe droughts in Iran in the early 2000s that lead to depleting rivers and lakes (Agrawala et al. 2001), therefore changing land-cover types.

It is also worth looking at the areas where temperature limitation has increased, as is the case in the second quarter in eastern Australia and western Canada. Jacobs et al. (2013) found that eastern Australia did not show a significant annual warming trend from 1979 to 2010 which makes a slight increase in temperature control intra-annually plausible. Additionally, they found a cooling trend in eastern Australian during La Niña episodes. However, their analysis is also based on ERA Interim data, like the climatic control data in the LAIre dataset, and should therefore be verified with an independent source.

For western Canada, the situation is very different. The literature unanimously shows an increase in mean, minimum and maximum temperatures for all seasons in this period (BC MoE, 2015; Beaubien & Freeland, 2000; Bonsal & Prowse, 2003), making an actual increase in temperature limitation questionable. Closer inspection of the bimonthly climatic data from which the quarterly trends are aggregated shows that an increase in temperature control only showed up in 2 out of the 6 relevant 15-day periods from April to June, each in a slightly different, adjacent region. This increase in temperature control is therefore most likely an artifact of the interpolation of the ERA-Interim dataset and its aggregation into quarterly means and does not correspond to actual conditions on the ground.

### *Moisture*

The moisture-control trends showed a higher global variability than trends in temperature limitation, but most regions experienced a strong increase in moisture control of up to 10% per decade. As Matsoukas et al. (2011) note, part of the increase in control is due to the ERA Interim data on which the climatic controls are based, showing a faster rise in air temperature  $T$  than the rise in dew point temperature  $T_d$ , leading to increasing estimates for VPD. This would suggest that at least some of the observed increase in VPD control might not correspond to actual changes in VPD on the ground. The variations and very strong increases in VPD control in some regions do suggest

though that changes in VPD are not only due to a general increase in the difference of  $T$  to  $T_a$  from the climatic data. This means other factors are at play and a more in-depth analysis of the trends found here is indeed justified.

Many of the areas showing a strong increase in moisture control are semi-arid and arid regions, which are absolutely dominated by moisture control over most of the year. Increases in moisture-control can only happen in the winter months, where the moisture limitation is not yet at its maximum. This change may not have any effect on LSP since there is no vegetation; it is nonetheless an indicator of the further drying out of semi-arid and arid areas globally. No change was observed in the summer months, when moisture limitation is already 100%.

Interesting cases are the regions that are not dominated by moisture control but showed an increase in moisture limitation. This is the case in most of Europe for example, where an increase in moisture control particularly during the second quarter of the year was found, when plant growth rates are at a peak. Since this did not coincide with any change in annual dominating controls over the past 30 years, no visible effect on LSP is expected yet. However, if change rates remain at the current 5% per decade, an impact of moisture limitation on LSP could become noticeable in the coming decades. Strong increases in moisture control were also found in South America over all four quarters. This increase was likely amplified by several major drought events between the years 2000 and 2010 (Magalhães & Martins 2011). The impact of this change in control does, however, not correlate with LAI measurements (Anderson et al. 2015), suggesting that other biophysical parameters influenced phenology more than evaporative stress. Due to the droughts in the early 2000s, doing an analysis of trend breaks would be particularly useful here to assess the influence of short-term trends of climatic controls on LSP.

The decrease of moisture control in southern Africa and north-eastern Australia, which are dominated by moisture control over all 30 years, are also worth discussing. The effective decrease of VPD, or increase in available moisture, has been analysed in prior research for both regions based on modelled as well as remotely sensed data (Dorigo et al. 2012; Chen et al. 2014). While Dorigo et al. point out that precipitation is the main driver for the increase in southern African soil moisture, there is no clear consensus yet how precipitation and soil moisture influence each other in this region (Dorigo et al. 2012; Cook & Pau 2013) or how and how strongly ocean current anomalies such as the ENSO influence southern African precipitation and soil moisture (Reason & Jagadheesha 2005). More research is needed to understand these interactions and to understand their relevance for future trends in LSP.

#### 4.2.3 *Limitations of the climatic control model (extended GSI)*

Apart from the limitations regarding regional differences, which were discussed before, the model used for the climatic controls as well as the controls themselves have some known limitations. Firstly, the threshold-based Growing Season Index does not work equally well for all land-cover types, as Jolly et al. (2005) note. Stöckli et al. (2011) extended the model by setting different thresholds for temperature, VPD and radiation depending on the mix of Plant Functional Types (PFT) present in each pixel. While this adaptation allows for a more precise adaptation of the climatic controls model on a global scale, the PFTs used by Stöckli do not change over time. This introduces uncertainties in areas where a significant change in land-cover has occurred. An adaptive algorithm to deal with land-cover changes during the observation period would therefore be required to more accurately extract the climatic control factors.

A second uncertainty stems from unknown behaviour of most plants in a changing climate. While a linear-threshold model as used by Jolly might be adequate for current conditions, it has yet to be seen how well it works when temperature becomes less of a driver and moisture becomes a more important global limiting factor. Adding to that is the unknown evolutionary adaptive nature of plants in a changing climate. Studies for individual plants have shown rapid evolution in some species to cope with a changing environment (Franks et al. 2007), however very little is known about how most plants or whole ecosystems react to long-term changes in limiting climatic controls.

Looking at the three climatic factors used for this analysis, temperature and radiation can be considered direct measures of a limiting factor, while VPD cannot. As Jolly et al. (2005) note, VPD is used because it can be calculated easily and continuously. They also remark however that plant-climate interactions influencing VPD are complicated and ask appropriately: “does VPD influence phenology or does phenology influence VPD?” A better understanding of the complex nature of the VPD in the climate-LSP model is needed to really understand the impact of the changes observed in this thesis, and how they might affect LSP in the future.

### 4.3 Influence of Climatic Controls on LSP

In this chapter, results from all three research questions are combined to analyse the impact of changes in climatic controls in the 30 days prior to Start and End of Season.

#### 4.3.1 *Dominating Controls at SOS and EOS*

When comparing dominating controls at Start and End of Season, big differences are visible in the spatial distribution of the controls. During SOS the pattern of dominating controls is very similar to the pattern found in yearly dominating controls (chapter

3.2.1). This is in strong contrast to the dominating controls at EOS, which show a completely different spatial distribution, particularly for the Northern Hemisphere. Differences can also be found when looking at the temporal variability of dominating controls during SOS and EOS. For the SOS, the changes over time were small and located at the borders of different dominating controls. For EOS on the other hand, large scale changes in dominance were found from year to year, particularly for the Northern Hemisphere, but also in southern Africa and South America.

#### 4.3.2 Start of Season in the Northern Hemisphere

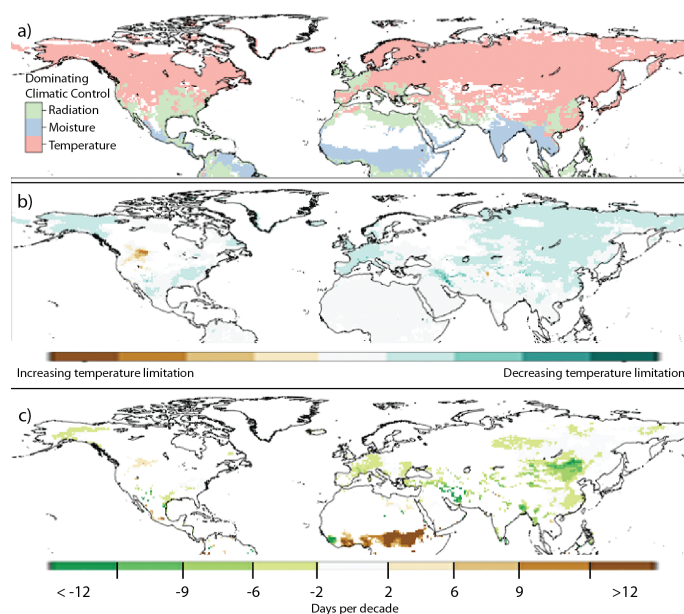


**Fig. 18:** Comparison of (a) dominating controls at SOS, (b) changes in the temperature limitation during the second quarter of the year and (c) decadal change of SOS from 1982 – 2011.

For the Start of Season in the Northern Hemisphere, the temperature domination coupled with decrease of temperature control observed in the second quarter results in an earlier SOS (see section 4.2 and 4.1 respectively). This is a strong indication that temperature was and still is the main driver for plant growth for the Northern Hemisphere, as has been the general consensus in the literature (Jeong et al. 2011; Badeck et al. 2004). This is

further confirmed by the trend analysis of temperature control during Start of Season. It shows very little change during SOS for most of the Northern Hemisphere, implying that the SOS and minimum temperature change at similar rates (Fig. 19) since minimum temperature directly drives SOS. Exceptions are Scandinavia, Britain, Central Asia as well as China, where influence of temperature control is getting smaller during SOS. This would imply other processes, either climatic or anthropogenic, started having a bigger influence on SOS during the last 30 years in those regions.

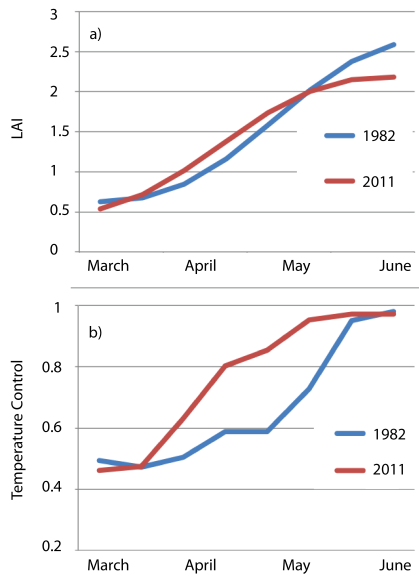


**Fig. 19:** Shift in temperature control (a) and LAI (b) from March to June for 1982 and 2011 towards an earlier date in the Northern Hemisphere.

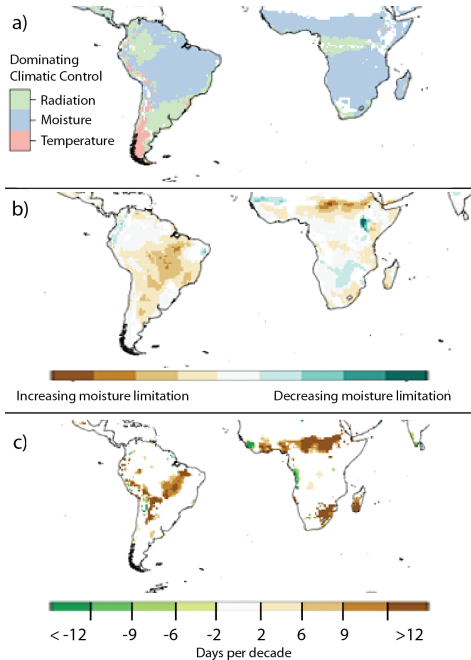


**Fig. 20:** Comparison of (a) dominating controls at SOS, (b) changes in moisture limitation in the 3<sup>rd</sup> quarter and (c) decadal change of SOS from 1982 – 2011 for South America and Africa.

With rising temperatures and earlier SOS onset, other factors might start having a stronger impact on the Start of Season. As expected, the trend analysis during SOS showed that radiation is an increasingly limiting factor since the SOS moves towards earlier dates and therefore to days with fewer hours of daylight. It could be expected to see an increase in moisture control at Start of Season as well due to the rising importance of the moisture control in spring in the Northern Hemisphere as seen in section 4.2. This was however not the case in the trend analysis. The moisture control factor does neither increase nor decrease at SOS, while the SOS shifts to an earlier date. This counterintuitive finding is important since it shows the consequence of connecting LSP to climatic controls, rather than just looking at climatic factors by quarter as done in section 4.2.

#### 4.3.3 Start of Season in the Southern Hemisphere

For South America, a similar analysis at SOS as in the Northern Hemisphere can be done. By looking at a combination of dominating controls at SOS, change of moisture in the third and fourth quarter of the year and the shift in SOS during that time (Fig. 10 and Fig. 20), one can find that the shift in SOS towards a later date might be explained by the change in moisture limitation. Moisture is the dominating factor for the affected region and showed an increase in control over the 30 years. With this increase in moisture limitation, a later onset of the growing season was observed. This

dependence on moisture has already been shown for seasonal behaviour for certain forest types in Brazil (Funch et al. 2002) but not in a long-range and large-scale trend analysis such as this thesis. Changes in moisture availability and LSP due to large-scale logging in the Brazilian Amazon rainforest which were found based on MODIS time-series analysis (Koltunov et al. 2009) could not be seen in the analysis on this larger spatial and temporal scale. While some change in moisture in the Amazonian rainforest can be seen, a large part of the major increase in moisture control is outside of the rainforest and its causes are therefore likely not directly connected to logging. Similar to the anthropogenic changes observed in China, the changes in LSP caused by logging themselves are most likely not as clear in the modelled data since the LAIre does not take into account changes in land-cover as discussed in section 4.1.

A similar situation to Brazil can be seen in the south-eastern tip of Africa, where the SOS also showed a trend towards a later date of year in the moisture-control dominated area. While the changes in moisture control observed during the third and fourth quarter of the year (see Fig. 10 and Fig. 20) are very small, the trend analysis for the 30-day period prior to SOS shows a clear increase in moisture while temperature and light controls go down due to the delay of SOS. However, in both South America and south-eastern Africa it cannot be clearly determined if moisture is the driving force behind the change, or if the change in moisture is influenced by the change of SOS (see discussion of VPD in previous section and Jolly et al. 2005).

#### *4.3.4 End of Season in the Northern Hemisphere*

Due to inter-annual variability of dominating controls during the End of Season, analysing the impact of the dominant climatic control in that period is not as straightforward as for Start of Season. Because of the frequent changes in dominating control from year to year, connecting the changes of limiting climatic controls to changes in date of EOS cannot be done. For the Northern Hemisphere in particular, the high variability of dominating controls over the years could be an indication that the climatic factors influencing the End of Season are more complicated and multi-faceted than the temperature dominated Start of Season.

However, it could also be an indication that the driving climatic limitations for End of Season occur earlier than the 30-day period examined in this thesis. For the Northern Hemisphere this seems to be the case according to Jeong et al. (2011) who found that temperature related effects initiating the End of Season can occur up to 4 months before actual EOS. This finding is supported by the analysis of individual trends of climatic controls during EOS. A strong increase in moisture control was observed for most of the

Northern Hemisphere, which counters the finding that EOS shows a delay for much of the Northern Hemisphere particularly in the past 10 years. Therefore it must be concluded that there is no indication of changes of control at EOS affecting the date of EOS during the past 30 years.

Nonetheless, the big variations in dominating climatic control factors during EOS could be the key to help explain why the EOS delay has a strong contribution to the overall GSL changes (Jeong et al. 2011; Garonna et al. 2014). The high temporal and spatial variability in dominating controls during EOS also indicate that a more regional analysis based on regional climate models is needed to understand the exact effects on plant senescence. Also, the large-scale increase in moisture control for the Northern Hemisphere might become an important control for the EOS in the future and should be given particular attention in further research.

#### *4.3.5 End of Season in the Southern Hemisphere*

In the Southern Hemisphere, the annual variability of dominating controls during EOS is not as high as in the Northern Hemisphere. The dominating climatic limitation for most areas was radiation, however. Changes in radiation limitation are a result rather than a driver of the shift in EOS, because radiation is mainly a factor of day-length and is therefore not influenced by a changing climate. This makes changes in EOS much harder to analyse, since the dominant control factor cannot be used to explain trends.

When looking at individual trends in climatic controls however, an increase in moisture control is observed particularly for South America. Just like the Northern Hemisphere, this does not translate into observable changes of EOS for the 30 years analysed.

However, moisture was the only of the three controls to change significantly in South America during the last 30 years and it could therefore be expected to become an increasingly important factor for the future.

The decrease in moisture control observed for southern Africa coincides with a delay of EOS, expanding findings from section 4.2 and pointing to a more important role of moisture limitation during EOS rather than SOS, where an increase in moisture control did not lead to significant changes of the SOS date. This further supports the recent scientific change of perspective to not only concentrate on the SOS but also study changes in EOS more thoroughly (Garonna et al. 2014; Jeong et al. 2011).

#### *4.3.6 Limitations*

A big limitation of this analysis is the focus on only 30 days prior to SOS and EOS. While it allows for a general assessment of the effects climatic controls might have on Start and

End of Season, it does not take into account climatic changes that happen outside this 30-day window. Particularly for EOS this might prove to be an important next step of the analysis performed here. Since the EOS generally showed too much variability in dominating controls to find conclusive influences of climatic controls on LSP, it seems likely that drivers of changes in EOS can be found several months before actual EOS (Jeong et al. 2011).

The big challenge in the study of LSP and climate interactions remains the development of quantifiable measures of influence of climate to LSP (Richardson et al. 2013). While this thesis tried to find ways to quantify changes in climatic controls over the past 30 years, understanding the exact effects of these changes on LSP remains difficult. Since only absolute changes for individual controls were analysed, it is not possible to assess the change of relative limitations. Further research, taking into account these relative differences and changes in relative importance, is needed to better understand the processes that drive global LSP. Quantifying LSP-climate interactions requires a good understanding of the underlying processes, yet to study those on a global scale, quantifiable metrics of this interaction are needed. Hence it has to be acknowledged that LSP-climate research is an iterative process by necessity.

Another limitation is that of scale dependency. This thesis approached the topic on a global scale and as such could only take into account large-scale phenomena. It became clear that certain regions particularly in the Southern Hemisphere and the tropics require a smaller-scale analysis to get a better understanding of the processes underlying trends in LSP. For the Northern Hemisphere however, the approach presented here corresponds well to regional analyses and has potential to explain large-scale effects of climate change on LSP.

Lastly, the thesis looked at linear trends within a fixed 30-year window from 1982–2011, which might overlook important short-term or recent trend changes, as reported for the Northern Hemisphere for the period of 2000 to 2010 for example (Jeong et al. 2011). The importance of trend breaks in the analysis of LSP time-series has been discussed in scientific literature before and algorithms to find those trend breaks have been developed (de Jong et al. 2012). A next step would therefore be to build on the approach presented here and account for such trend breaks to get a more accurate picture of global change of climatic controls and LSP.

## 5 Conclusion and Outlook

The first research question of how well LSP parameters extracted from the modelled and measured LAI compare with each other was answered by correlating the LAI<sub>r</sub> developed by Stöckli et al. (2011) to the remotely sensed LAI<sub>3g</sub>. The comparison showed that realistic LAI data can be computed with a phenological model based on climatic controls. LSP parameters extracted from the dataset compared well to LSP parameters extracted from the measured dataset, particularly the Start of Season in the Northern Hemisphere. This not only allows for an analysis of historical LSP trends based on the three underlying climatic controls of temperature, VPD and incoming radiation, but it also opens up the possibility of modelling future LSP scenarios by using data from global or regional climate models to model LAI. The End of Season showed bigger variability between the two datasets, which suggests that the processes underlying autumn phenology need to be better understood before accurate models and predictions can be made.

To address the second research question of how climatic controls have changed over the last 30 years, the inter-annual changes of climatic controls were examined. The time-series of dominating climatic controls from 1982–2011 showed that Brazil experienced a large-scale change from radiation limitation to moisture limitation over the past 30 years. For other regions, inter-annual variability along ecotones was observed without clear long-term changes of domination from one control to another. The individual strength of VPD and temperature control on the other hand have shown significant global change, with temperature showing a global decrease in impact as a limiting factor on plant growth, while VPD is showing a global increase as a limiting factor.

The third research question was addressed by extracting climatic controls in the 30 days prior to Start and End of Season to study changes influencing plant growth and senescence. The dominating controls during Start of Season were shown to be much more stable than those during End of Season, indicating a more complex LSP-climate interaction during EOS, compared to SOS. Individual analysis of climatic controls showed a global increase in moisture-control limitation, affecting the Northern Hemisphere during EOS and the Southern Hemisphere during SOS. Temperature was shown to decrease in influence globally during SOS, and for the Northern Hemisphere during EOS. Radiation-limitation increased in at SOS for the Northern Hemisphere and decreased in control for much of the Southern Hemisphere due to the shift in SOS.

Most studies on the global impact of climate change on LSP are focused on temperature as a main driver of plant phenology. The findings presented here suggest that with rising temperatures, moisture and radiation will most likely become more important global limiting factors for LSP in the near future. It has been pointed out before (Richardson et al. 2013) that in order to assess the effects of this change, underlying processes need to be better understood and quantitative metrics of these phenology-climate interactions need to be developed. Particular focus should be put on understanding End of Season processes to more accurately represent the EOS in phenology models.

## References

- Agrawala, S., Barlow, M., Cullen, H., & Lyon, B. (2001). *The Drought and Humanitarian Crisis in Central and Southwest Asia : A Climate PerScience, Linking spective*. IRI Social Report NO. 01-11. New York.
- Anderson, M. C., Zolin, C., Hain, C. R., Semmens, K., Tugrul Yilmaz, M., & Gao, F. (2015). Comparison of satellite-derived LAI and precipitation anomalies over Brazil with a thermal infrared-based Evaporative Stress Index for 2003-2013. *Journal of Hydrology*, 526, 287–302.
- Anwar, M. R., Liu, D. L., Farquharson, R., Macadam, I., Abadi, A., Finlayson, J. (2015). Climate change impacts on phenology and yields of five broadacre crops at four climatologically distinct locations in Australia. *Agricultural Systems*, 132, 133–144.
- Anyamba, a., & Tucker, C. J. (2005). Analysis of Sahelian vegetation dynamics using NOAA-AVHRR NDVI data from 1981-2003. *Journal of Arid Environments*, 63(3), 596–614.
- Badeck, F. W., Bondeau, A., Böttcher, K., Doktor, D., Lucht, W., Schaber, J., & Sitch, S. (2004). Responses of spring phenology to climate change. *New Phytologist*, 162(2), 295–309.
- Baret, F., Hagolle, O., Geiger, B., Bicheron, P., Miras, B., Huc, M. (2007). LAI, fAPAR and fCover CYCLOPES global products derived from VEGETATION. Part 1: Principles of the algorithm. *Remote Sensing of Environment*, 110(3), 275–286.
- BC MoE (2015). *Indicators of Climate Change for British Columbia 2015 Update*. British Columbia Ministry of Environment. Vancouver, Canada. Retrieved from: <http://www2.gov.bc.ca/assets/gov/environment/climate-change/policy-legislation-and-responses/adaptation/climatechangeindicators-2015update.pdf> [28 August 2015]
- Beaubien, E. G., & Freeland, H. J. (2000). Spring phenology trends in Alberta, Canada: links to ocean temperature. *International Journal of Biometeorology*, 44(2), 53–59.
- Bonsal, B. R., & Prowse, T. D. (2003). Trends and variability in spring and autumn 0 degrees C-isotherm dates over Canada. *Climatic Change*, 57(3), 341–358.
- Cao, K. H., & Birchenall, J. a. (2013). Agricultural productivity, structural change, and economic growth in post-reform China. *Journal of Development Economics*, 104, 165–180.
- Carlson, T. N., & Ripley, D. a. (1997). On the relation between NDVI, fractional vegetation cover, and leaf area index. *Remote Sensing of Environment*, 62(3), 241–252.
- Chen, J. M., & Black, T. A. (1992). Defining leaf area index for non-flat leaves. *Plant, Cell and Environment*, 15(4), 421–429.

- Chen, T., de Jeu, R. a M., Liu, Y. Y., van der Werf, G. R., & Dolman, a. J. (2014). Using satellite based soil moisture to quantify the water driven variability in NDVI: A case study over mainland Australia. *Remote Sensing of Environment*, *140*, 330–338.
- Cook, B., & Pau, S. (2013). A Global Assessment of Long-Term Greening and Browning Trends in Pasture Lands Using the GIMMS LAI3g Dataset. *Remote Sensing*, *5*(5), 2492–2512.
- Dardel, C., Kergoat, L., Hiernaux, P., Mougin, E., Grippa, M., & Tucker, C. J. (2014). Re-greening Sahel: 30 years of remote sensing data and field observations (Mali, Niger). *Remote Sensing of Environment*, *140*, 350–364.
- De Jong, R., de Bruin, S., de Wit, A., Schaepman, M. E., & Dent, D. L. (2011). Analysis of monotonic greening and browning trends from global NDVI time-series. *Remote Sensing of Environment*, *115*(2), 692–702.
- De Jong, R., Verbesselt, J., Schaepman, M. E., & de Bruin, S. (2012). Trend changes in global greening and browning: Contribution of short-term trends to longer-term change. *Global Change Biology*, *18*(2), 642–655.
- Dorigo, W., De Jeu, R., Chung, D., Parinussa, R., Liu, Y., Wagner, W., & Fernández-Prieto, D. (2012). Evaluating global trends (1988-2010) in harmonized multi-satellite surface soil moisture. *Geophysical Research Letters*, *39*(17), 3–9.
- Fang, H., Wei, S., & Liang, S. (2012). Validation of MODIS and CYCLOPES LAI products using global field measurement data. *Remote Sensing of Environment*, *119*, 43–54.
- Fernandes, R., Plummer, S., Nightingale, J., Baret, F., Camacho, F., Fang, H., Garrigues, S., Gobron, N., Lang, M., Lacaze, R., LeBlanc, S., Meroni, M., Martinez, B., Nilson, T., Pinty, B., Pisek, J., Sonnentag, O., Verger, A., Welles, J., Weiss, M., & Widlowski, J.L. (2014). Global Leaf Area Index Product Validation Good Practices. Version 2.0. In G. Schaepman-Strub, M. Román, & J. Nickeson (Eds.), *Best Practice for Satellite-Derived Land Product Validation* (p. 76): Land Product Validation Subgroup (WGCV/CEOS)
- Foody, G. M. (2001). Monitoring the magnitude of land-cover change around the southern limits of the Sahara, (July). Retrieved from <http://www.asprs.org/publications/pers/2001journal/july/abstracts.html#841>
- Franks, S. J., Sim, S., & Weis, A. E. (2007). Rapid evolution of flowering time by an annual plant in response to a climate fluctuation. *Proceedings of the National Academy of Sciences of the United States of America*, *104*(4), 1278–1282.
- Funch, L. S., Funch, R., & Barroso, G. M. (2002). Phenology of gallery and montane forest in the Chapada Diamantina, Bahia, Brazil. *Biotropica*, *34*(1), 40–50.
- Garonna, I., de Jong, R., de Wit, A. J. W., Múcher, C. a, Schmid, B., & Schaepman, M. E. (2014). Strong contribution of autumn phenology to changes in satellite-derived growing season length estimates across Europe (1982-2011). *Global Change Biology*, *20*(11), 3457–70.

- Garonna, I.; de Jong, R. & Schaepman, M.E., Variability and evolution of global land surface phenology over the past three decades (1982-2012), submitted to: *Global Change Biology*.
- GCOS (2011). Systematic Observation Requirements For Satellite-Based Data Products for Climate - 2011 Update, World Meteorological Organization (WMO), Geneva, Switzerland.
- Ghasemi, A. R. (2015). Changes and trends in maximum, minimum and mean temperature series in Iran. *Atmospheric Science Letters*, 16(3), 366–372.
- Gouveia, C., Trigo, R. M., DaCamara, C. C., Libonati, R., & Pereira, J. M. C. (2008). The North Atlantic Oscillation and European vegetation dynamics. *International Journal of Climatology*, 28(14), 1835–1847.
- IPCC (2014). *Climate Change 2014: Synthesis Report. Contribution of Working Groups I, II and III to the Fifth Assessment Report of the Intergovernmental Panel on Climate Change [Core Writing Team, R.K. Pachauri and L.A. Meyer (eds.)]*. IPCC. Geneva, Switzerland.
- Jacobs, S. J., Pezza, A. B., Barras, V., Bye, J., & Vihma, T. (2013). An analysis of the meteorological variables leading to apparent temperature in Australia: Present climate, trends, and global warming simulations. *Global and Planetary Change*, 107, 145–156.
- Jeong, S.-J., Ho, C.-H., Gim, H.-J., & Brown, M. E. (2011). Phenology shifts at start vs. end of growing season in temperate vegetation over the Northern Hemisphere for the period 1982-2008. *Global Change Biology*, 17(7), 2385–2399.
- Jiang, B., Liang, S., Wang, J., & Xiao, Z. (2010). Modeling MODIS LAI time series using three statistical methods. *Remote Sensing of Environment*, 114(7), 1432–1444.
- Jiang, Z., Huete, A. R., Chen, J., Chen, Y., Li, J., Yan, G., & Zhang, X. (2006). Analysis of NDVI and scaled difference vegetation index retrievals of vegetation fraction. *Remote Sensing of Environment*, 101(3), 366–378.
- Jin, H., & Eklundh, L. (2014). A physically based vegetation index for improved monitoring of plant phenology. *Remote Sensing of Environment*, 152, 512–525.
- Jolly, W. M., Nemani, R., & Running, S. W. (2005). A generalized, bioclimatic index to predict foliar phenology in response to climate. *Global Change Biology*, 11(4), 619–632.
- Julien, Y., & Sobrino, J. a. (2009). Global land surface phenology trends from GIMMS database. *International Journal of Remote Sensing*, 30(13), 3495–3513.
- Koltunov, A., Ustin, S. L., Asner, G. P., & Fung, I. (2009). Selective logging changes forest phenology in the Brazilian Amazon: Evidence from MODIS image time series analysis. *Remote Sensing of Environment*, 113(11), 2431–2440.

- Magalhães, A. R., & Martins, E. S. (2011). Drought and Drought Policy in Brazil. In M. V. K. Sivakumar, R. P. Motha, D. A. Wilhite, & J. J. Qu (Eds.), *Towards a Compendium on National Drought Policy: Proceedings of an Expert Meeting* (p. 135pp). Washington, DC: World Meteorological Organization.
- Matsoukas, C., Benas, N., Hatzianastassiou, N., Pavlakis, K. G., Kanakidou, M., & Vardavas, I. (2011). Potential evaporation trends over land between 1983-2008: Driven by radiative fluxes or vapour-pressure deficit? *Atmospheric Chemistry and Physics*, *11*(15), 7601–7616.
- Mishra, N. B., Crews, K. a., Neeti, N., Meyer, T., & Young, K. R. (2015). MODIS derived vegetation greenness trends in African Savanna: Deconstructing and localizing the role of changing moisture availability, fire regime and anthropogenic impact. *Remote Sensing of Environment*, *169*, 192–204.
- Myneni, R. B., Hall, F. G., Sellers, P. J., & Marshak, a. L. (1995). The Interpretation of Spectral Vegetation Indexes. *IEEE Transactions on Geoscience and Remote Sensing*.
- Pinzon, J. E., & Tucker, C. J. (2014). A non-stationary 1981-2012 AVHRR NDVI3g time series. *Remote Sensing*, *6*(8), 6929–6960.
- Reason, C. J. C., & Jagadheesha, D. (2005). A model investigation of recent ENSO impacts over southern Africa. *Meteorology and Atmospheric Physics*, *89*(1-4), 181–205.
- Reed, B., White, M., & Brown, J. (2003). Remote Sensing Phenology. In M. Schwartz (Ed.), *Phenology: An Integrative Environmental Science SE - 23* (Vol. 39, pp. 365–381). Springer Netherlands.
- Richardson, A. D., Anderson, R. S., Arain, M. A., Barr, A. G., Bohrer, G., Chen, G.(2012). Terrestrial biosphere models need better representation of vegetation phenology: results from the North American Carbon Program Site Synthesis. *Global Change Biology*, *18*(2), 566–584.
- Richardson, A. D., Keenan, T. F., Migliavacca, M., Ryu, Y., Sonnentag, O., & Toomey, M. (2013). Climate change, phenology, and phenological control of vegetation feedbacks to the climate system. *Agricultural and Forest Meteorology*, *169*, 156–173.
- Roerink, G. J., Menenti, M., Soepboer, W., & Su, Z. (2003). Assessment of climate impact on vegetation dynamics by using remote sensing. *Physics and Chemistry of the Earth*, *28*(1-3), 103–109.
- Roerink, G. J., Menenti, M., & Verhoef, W. (2000). Reconstructing cloudfree NDVI composites using Fourier analysis of time series. *International Journal of Remote Sensing*, *21*(9), 1911–1917.
- Rouse, J. W., Haas, R. H., Schell, J. a., & Deering, D. W. (1973). Monitoring the Vernal Advancement and Retrogradation (Green Wave Effect) of Natural Vegetation. *N.G.T.I.F. Report (Ed.)*, 112.
- Saboohi, R., Soltani, S., & Khodaghali, M. (2012). Trend analysis of temperature parameters in Iran. *Theoretical and Applied Climatology*, *109*(3-4), 529–547.

- Schwartz, M. D. (1999). Advancing to full bloom: planning phenological research for the 21st century. *International Journal of Biometeorology*, 42(3), 113–118.
- Stöckli, R., Rutishauser, T., Baker, I., Liniger, M. a., & Denning, a. S. (2011). A global reanalysis of vegetation phenology. *Journal of Geophysical Research*, 116(G3), G03020.
- Tucker, C. J. (1979). Red and photographic infrared linear combinations for monitoring vegetation. *Remote Sensing of Environment*, 8(2), 127–150.
- Tucker, C., Pinzon, J., Brown, M., Slayback, D., Pak, E., Mahoney, R. (2005). An extended AVHRR 8-km NDVI dataset compatible with MODIS and SPOT vegetation NDVI data. *International Journal of Remote Sensing*, 26(20), 4485–4498.
- Verger, A., Baret, F., Weiss, M., Filella, I., & Peñuelas, J. (2015). GEOCLIM: A global climatology of LAI, FAPAR, and FCOVER from VEGETATION observations for 1999–2010. *Remote Sensing of Environment*, 166, 126–137.
- White, M. a., de BEURS, K. M., Didan, K., Inouye, D. W., Richardson, A. D., Jensen, O. P., (2009). Intercomparison, interpretation, and assessment of spring phenology in North America estimated from remote sensing for 1982-2006. *Global Change Biology*, 15(10), 2335–2359.
- Zhao, J., Li, J., Liu, Q., & Yang, L. (2012). a Preliminary Study on Mechanism of Lai Inversion Saturation. *ISPRS - International Archives of the Photogrammetry, Remote Sensing and Spatial Information Sciences*, XXXIX-B1(September), 77–81.
- Zhu, Z., Bi, J., Pan, Y., Ganguly, S., Anav, A., Xu, L., (2013). Global Data Sets of Vegetation Leaf Area Index (LAI)3g and Fraction of Photosynthetically Active Radiation (FPAR)3g Derived from Global Inventory Modeling and Mapping Studies (GIMMS) Normalized Difference Vegetation Index (NDVI3g) for the Period 1981 to 2. *Remote Sensing*, 5(2), 927–948.

## Acknowledgements

I would like to thank the following people who helped me in the course of this thesis: First and foremost my two main supervisors, Rogier de Jong and Irene Garonna, who not only supported me with great feedback and ideas throughout the working process, but also offered me insights and advice far beyond the master thesis. They also gracefully put up with a student who decided to put his master thesis on hold for 3 months to pursue an internship in another country – for which I am extremely grateful. Sincere thanks also go to Reto Stöckli of MeteoSchweiz, who created the reanalysed LAI dataset used in this thesis and who gave valuable inputs during the final phase of this thesis. Last but not least my thanks go to my fellow master thesis writer Claudio Henry, who was always there to talk about the writing process, compare progress and share the aches and pains that go with working on and writing a master thesis.

## Appendix A: Code used for processing

All the code produced and used to process the data can be found on

<https://github.com/dschenkel/geo511-code>. Not included are the files for HANTS processing as well as the algorithm used to extract LSP parameters, as the rights to those are with the respective authors. The file structure is as follows:

- IDL/
  - *IDL Scripts used for extracting individual yearly files (split in northern and Southern Hemisphere) for LAI3g, initialize HANTS processing, resampling LAI3g to match spatial resolution of LAIre*
- R/
  - *R-Scripts used for further data processing and statistical analysis*
- R/general\_funtions.R
  - *Functions used in many scripts such as statistical analyses (linear regression, print scatter plot) as well as trend analysis*
- R/quickplot.R
  - *Functions to easily classify and plot maps*
- R/0\_LSP-extraction\_implementation/
  - *My own implementation used to extract LSP parameters (not used in final processing)*
- R/0\_preprocessing
  - *Scripts used for data-preprocessing such as setting LAI3g no-value pixels to 0 (for resampling)*
- R/0\_preprocessing/resize/
  - *Scripts used to resize LAIre temporally (daily to bimonthly)*
- R/0\_preprocessing/watermask/
  - *Scripts used to create watermasks from LAIre and LAI3g*
- R/1\_LAI\_comparison
  - *Scripts used to correlate and compare the two LAI datasets, get trends and plot results*
- R/2\_climaticcontrols
  - *Scripts used to extract climatic controls, do a trend analysis and extract dominating controls*
- R/3\_cc-LAI
  - *Files used to extract climatic controls at SOS/EOS, define dominating controls and do trend analysis*

## Appendix B: Parameterization for HANTS-processing

To smooth the dataset, the HANTS algorithm (version 1.3) developed by Wout Verhoefen and implemented in IDL by Allard de Wit was used. HANTS uses an iterative approach: It applies a Fast Fourier Transform (FFT) to the time-series to extract pre-defined low-order Fourier frequencies. Then it is transformed back (inverse, iFFT) to compare the resulting profile with the original one and repeat the process if any values are still outside the Fit-Error-Tolerance (FET). The iterative process is stopped when all values are within the FET or when iMax (maximum iterations) is reached. Parameters used are described in table B.1.

**Table B.1:** Parameters for HANTS processing. Differences for LAIre and LAI3g are due to the different ranges (LAI3g values are 10-times bigger than LAIre).

Parameter	Value	Additional Description
Fit-Error-Tolerance (FET)	0.7 (LAIre) 7 (LAI3g)	Maximum deviation between fitted Fourier curve and LAI values
Frequencies	0, 1, 2, 3	n-order frequencies to be extracted. 0-3 were chosen to be able to differentiate multiple growing seasons within a year while still getting a smooth profile
Range	-2 – 8 (LAIre) -2 –80 (LAI3g)	Maximum range of LAI values. Values outside this range get excluded
Throw-Away-Threshold (TAT)	10	Maximum number of observations that can be discarded (for outliers)
iMax	6	Maximum number of iterations before smoothing is stopped

## Personal Declaration

I hereby declare that the submitted thesis is the result of my own, independent work. All external sources are explicitly acknowledged in the thesis.

David Schenkel

Oberglatt, 24 September 2015